Bioorganic Chemistry xxx (xxxx) xxx

Contents lists available at ScienceDirect

Bioorganic Chemistry

journal homepage: www.elsevier.com/locate/bioorg

Generation of potent Nrf2 activators *via* tuning the electrophilicity and steric hindrance of vinyl sulfones for neuroprotection

Zi-Long Song, Yanan Hou, Feifei Bai, Jianguo Fang *

State Key Laboratory of Applied Organic Chemistry & College of Chemistry and Chemical Engineering, Lanzhou University, China

ARTICLE INFO

Keywords:
Oxidative stress
Vinyl sulfone
Antioxidant
Nrf2
Neuroprotection

ABSTRACT

Oxidative stress is constantly involved in the etiopathogenesis of an ever-widening range of neurodegenerative diseases. As a consequence, effective repression of cellular oxidative stress to a redox homeostatic condition is a promising and feasible strategy to treat, or at least retard the progression of, such disorders. Nrf2, a primary orchestrator of cellular antioxidant response machine, is responsible for detoxifying and compensating for deleterious oxidative stress *via* transcriptional activation of a diverse array of antioxidant biomolecules. In the framework of our persistent interest in disclosing small molecules that interfere with cellular redox-regulating machinery, we report herein the synthesis, optimization, and biological assessment of 47 vinyl sulfone scaffold-bearing small molecules, most of which exhibit robust neuroprotective effect against H_2O_2-mediated lesions to PC12 cells. After initial screening, the most potent neuroprotective compounds **9b** and **9c** with marginal cytotoxicity were selected for the follow-up studies. Our results demonstrate that their neuroprotective effects are attributed to the up-regulation of a panel of antioxidant genes and corresponding gene products. Further mechanistic studies indicate that Nrf2 is indispensable for the cellular performances of **9b** and **9c**, arising from the fact that silence of Nrf2 gene drastically nullifies their protective action. Taken together, **9b** and **9c** discovered in this work merit further development as neuroprotective candidates for the treatment of oxidative stress-mediated pathological conditions.

1. Introduction

During various metabolic processes, aerobic organisms inevitably produce reactive oxygen species (ROS), such as hydrogen peroxide, superoxide anion and so on [1]. These vigorous species play both beneficial and deleterious roles in cells [1–3]. Under physiological conditions, ROS levels are under the control of antioxidant defense system, and ROS are of paramount importance in various repertoires of cellular signal transduction pathways [3,4]. However, once this equilibrium is beyond of control, due to the insufficient antioxidant response mechanism and/or excessive ROS generation, oxidative stress ensues [1,4]. Oxidative stress elicits a wealth of detrimental effects on cellular vital components, including proteins, lipids, and nucleic acids [1], and contributes to numerous pathological conditions, such as neurodegenerative disorders [5], cancers [6], digestive system diseases [7], and cardiovascular diseases [8].

Although the brains account for only 2 ~ 5% of whole body weight, they voraciously consume about 25 ~ 30% of oxygen budget needed for supporting the whole body [9]. Additionally, brains are equipped with high levels of transition metals, modest antioxidant response mechanism, and considerable amounts of polyunsaturated fatty acids [5,9,10], all of which predispose brain neurons particularly vulnerable to oxidative stress. Further, dopaminergic neurons might sustain an excessive overload of oxidative stress, emanating from metabolism of dopamine (DA) [11]. Enzymatic metabolism of DA by monoamine oxidase (MAO) produces H_2O_2 as a byproduct. Alternatively, spontaneous oxidation of DA leads to the generation of neuromelanin and dopamine quinones (DAQs) [12], both of which result in the formation of ROS *via* redox-cycling in the presence of reducing agents. In addition, DAQs could either be engaged in electrophilic addition with cysteine-containing proteins, nucleic acids, and thiol antioxidant glutathione (GSH) or undergo cyclization process to form highly unstable and reactive dopaminochrome that is also prone to redox-cycling through consecutive consumption of NADPH and concomitant release of superoxide anion [13]. These convergences of evidences suggest that the brains are extremely sensitive to oxidative stress that imparts cumulative damages on brain neurons. Besides, owing to the limited regenerative capacity of neurons resulting from their post-mitotic characteristic [5], progressive

* Corresponding author.
E-mail address: fangjg@lzu.edu.cn (J. Fang).

https://doi.org/10.1016/j.bioorg.2020.104520
Received 21 March 2020; Received in revised form 30 October 2020; Accepted 26 November 2020
Available online 30 November 2020

loss of brain neurons takes place, which leads to the development of various neurodegenerative diseases, such as Parkinson's disease (PD), Alzheimer disease (AD), and Huntington's disease (HD). As a consequence, efficient elimination of excessive ROS and restoring the homeostatic redox balance are intriguing and viable tactics to relieve the symptoms or even retard the progression of these pathological conditions [14–17]. Either exogenous or endogenous antioxidant molecules are able to neutralize noxious ROS; however, exogenous antioxidant molecules are usually characterized by short half-lives and narrow therapeutical windows, precluding their practical application in clinical studies [10]. Alternatively, activation of endogenous antioxidant response machinery is more preferred as such a process is able to exert sustainable beneficial effects through transcriptional up-regulation of a plethora of antioxidant species, such as thioredoxin reductase (TrxR), GSH, NAD(P)H quinone oxidoreductase 1 (NQO1), and heme oxygenase-1 (HO-1), all of which are referred as the "ultimate antioxidants" [18–20].

Nuclear factor erythroid 2-related factor 2 (Nrf2), a member of basic region leucine zipper transcription factors, belongs to Cap 'n' Collar (CNC) family and is a primary executor of the cellular antioxidative signaling network. An extensive range of intrinsic antioxidative species (*e.g.* TrxR, GSH, NQO1, and HO-1) are all governed by Nrf2 at transcriptional level [21]. Under physiological conditions, Nrf2 is maintained at a low basal level in quiescent cells, which is ascribed to its natural repressor Kelch-like ECH-associated protein 1 (Keap1) that retains Nrf2 in cytoplasm and sequentially shepherds it for degradation through the ubiquitination-proteasome pathway [22,23]. Once in the context of stressed conditions, a group of certain cysteine residues in Keap1 are modified, and the Keap1-mediated ubiquitination of Nrf2 is terminated. Sequentially, Nrf2 translocates and accumulates in nucleus, where it heterodimerizes with members of small musculoaponeurotic fibrosarcoma (sMAF) family of transcription factors, and binds to the regulatory enhancer sequences termed "antioxidant response element" (ARE) in the promoter region of many antioxidant genes, leading to the transcriptional activation of ARE-directed expression of abundant detoxifying/cytoprotective molecules [23–27]. In this regard, activation of endogenous antioxidant mechanism of Nrf2-ARE emerges to provide an inroad for therapeutical intervention, or at least delay of the progression, of neurodegenerative diseases [10,16–18,22,23,28–30].

During the last couple of decades, a broad range of researchers had paid intensive attention to the identification and development of Nrf2-ARE activators both from natural sources and synthetic community [18,22–26,31–35]. Delightedly, the well-known Nrf2 activator dimethyl fumarate (DMF, Tecfidera, Chart 1) has been already approved by the US Food and Drug Administration for the treatment of early multiple sclerosis (MS) *via* mitigating the oxidative stress in an Nrf2-dependent manner [36]. The successful clinical application of DMF also encourages our group to unveil more Nrf2-targeted molecules [37–47], and several naturally occurring molecules and synthetic agents have been found to exhibit potent Nrf2 activation capacity and thus show impressive neuroprotective effect [48–51] (Chart 1). Vinyl sulfone represents a chemical skeleton that is similar to α, β-unsaturated ketone (also renowned as Michael acceptor) shared with many Nrf2 activators [18,23,31] (Chart 1). Although several synthetic molecules bearing vinyl sulfone motif had been documented by sporadic studies to show neuroprotective activity [52–54], the molecular structural determinants responsible for this activity and the underlying mechanism are not entirely clarified. Herein, we report the synthesis, evaluation, and mechanistic studies of 47 vinyl sulfone derivatives as Nrf2 activators in protecting PC12 cells from H_2O_2-induced damages. Two compounds **9b** and **9c**, discovered through elaborate structural optimization, were identified to possess not only low cytotoxicity but also the highly neuroprotective activity, and therefore selected as hit compounds for further evaluation. The follow-up studies indicate that **9b** and **9c** could attenuate the H_2O_2-mediated insults *via* up-regulation of a wide range of antioxidant/detoxifying enzymes and molecules, including TrxR, GSH, NQO1, and HO-1. Further mechanistic studies reveal that activation of Nrf2 is imperative for the cellular physiological action of **9b** and **9c** in PC12 cells, since knock-down of Nrf2 expression almost abrogated the neuroprotection.

2. Results and discussion

2.1. Chemistry

A concise chemical conversion to the synthesis of intermediates and desired compounds was delineated in Scheme 1. First, intermediates **3** were obtained in high yields through a nucleophilic substitution reaction between commercially available materials **1** and **2**. Second, oxidation of intermediates **3** with 3-chloroperoxybenzoic acid (*m*-CPBA) gave the intermediates **4**. Finally, the Horner–Wadsworth–Emmons Reaction was employed to furnish the 47 target compounds in moderate to excellent yields *via* exploiting intermediates **4** and various easily accessible aromatic aldehydes as staring materials. All newly synthesized compounds were characterized through ^{1}H NMR (400 MHz), ^{13}C NMR (100 MHz), and ESI-MS analysis. Purity determination of all target

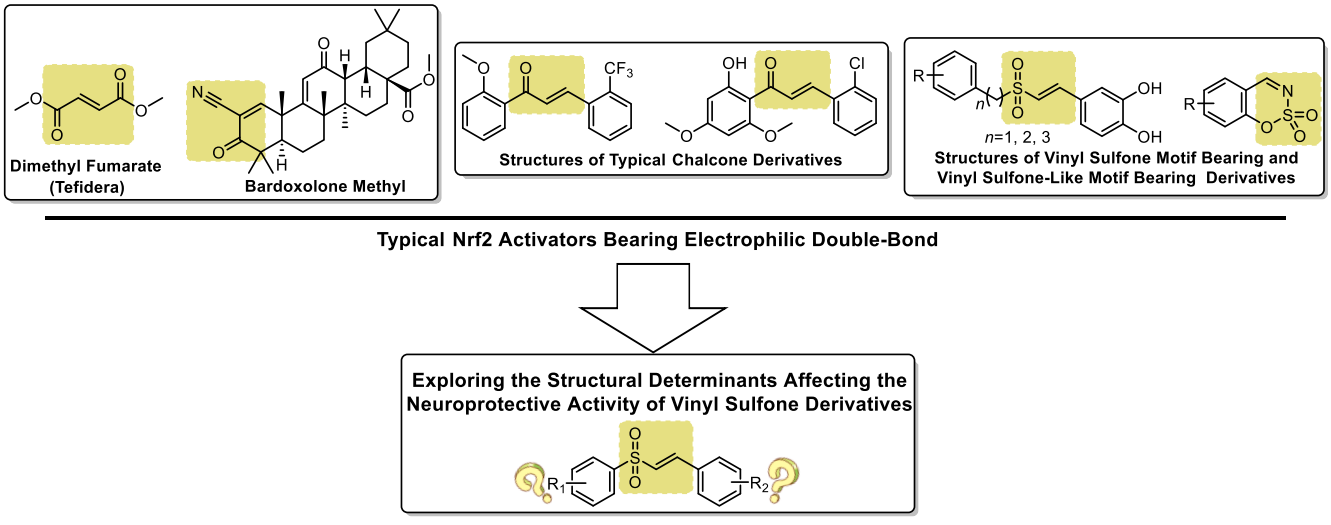

Chart 1. Previously reported Nrf2 activators and our strategy for the discovery of potent Nrf2 activators based on the electrophilic double-bond bearing vinyl sulfone scaffold.

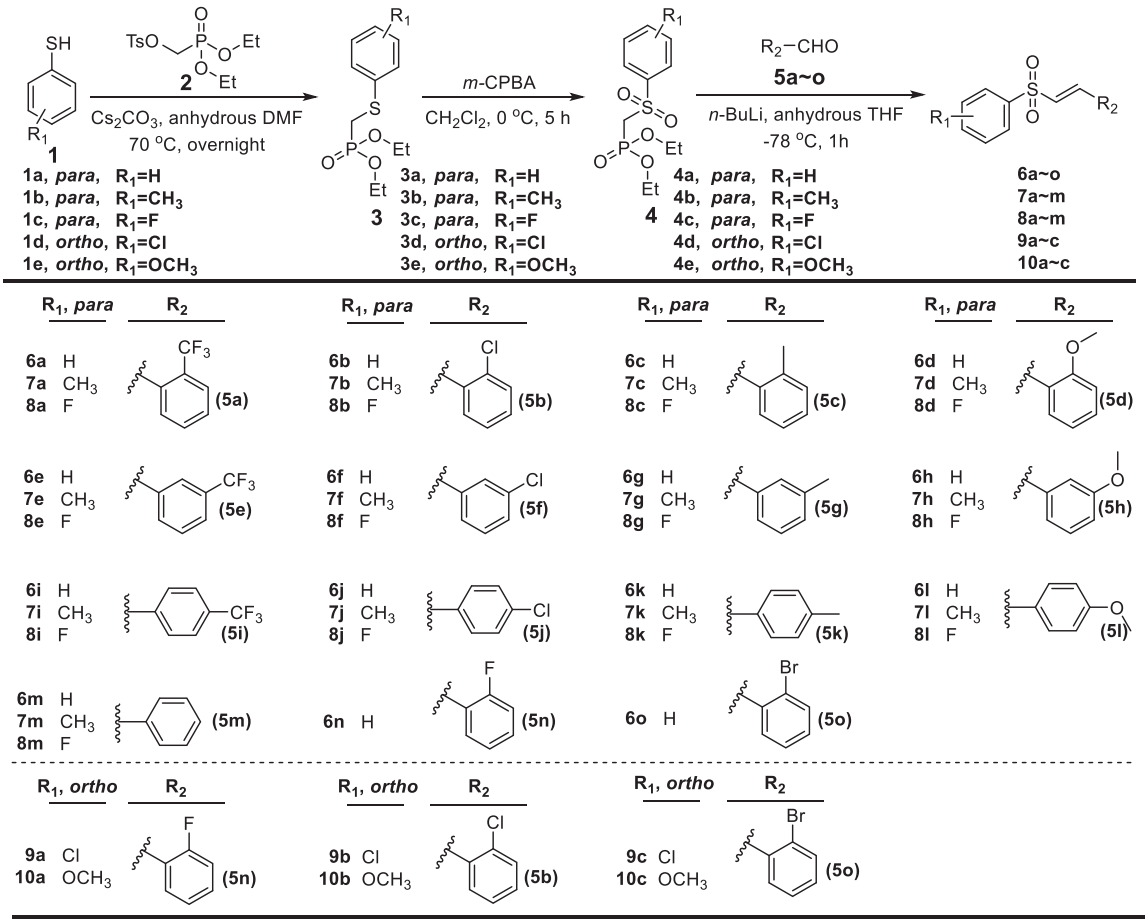

Scheme 1. Synthesis of intermediates and desired compounds.

compounds was analyzed by HPLC, and the purity (>95%) conform the *Journal* requirement and were suitable for further medicinal chemistry studies.

2.2. Biological studies

2.2.1. Initial screening, structure–activity relationship (SAR), and optimization studies

At the beginning of our research, 39 compounds were synthesized, namely **6a** ~ **m**, **7a** ~ **m**, and **8a** ~ **m**, and their cytotoxicity toward PC12 cells were assessed by the MTT assay. As exhibited in Fig. 1**A** (also shown as values in **Table S1** in Supporting Information), all the 39 compounds showed weak cytotoxicity, even at high concentration of 50 μM. As a consequence, these 39 compounds were all selected for the neuroprotective evaluation against H_2O_2-induced lesions to PC12 cells, a well-established cellular neurodegenerative diseases model. [24,39–41,53] The protection screening results (Fig. 1**B** and **Table S2** in Supporting Information) showed that 5 compounds (**6a** ~ **b**, **7b**, and **8a** ~ **b**) possessed apparent neuroprotective activity, with **6b** being the most potent one. As seen from these 5 most active compounds, the R_2 group should be an assembly with an electron-withdrawing atom/function group in close proximity to the vinyl group of the molecules, and the Cl atom is more preferred than the CF_3 group. On the other hand, activity determinants of the R_1 are complex, since the most active three compounds (**6b**, **7b**, and **8b**) have substituents as H (electron-neutral), CH_3 (slightly electron-donating), and F (electron-withdrawing). According to the results attained above and enlightened by studies performed previously by Park *et al.* [54], additional 8 compounds (**6n** ~ **o**, **9a** ~ **c**, and **10a** ~ **c**) were synthesized to further explore the SAR of R_1 and R_2 groups. The newly synthesized 8 compounds showed negligible cytotoxicity (Fig. 2**A** and **Table S3** in Supporting Information). Then, these 8 compounds plus **6b** were all evaluated for neuroprotection in the same model as that employed before. As shown in Fig. 2**B** (also shown as values in **Table S4** in Supporting Information), **6b** with R_1 = H is more neuroprotective than molecules (compounds **10a** ~ **c**) with R_1 = *ortho*-OCH_3 in neuroprotection. Further, compounds with R_1 = *ortho*-Cl shows more potent neuroprotective activity than their counterpart compounds with R_1 = H, respectively (**9b** > **6b**, **9c** > **6o**, and **9a** > **6n**, Fig. 3 and **Table S4** in Supporting Information). What's more, it is worth mentioning that R_2 = *ortho*-F might compromise the neuroprotective activity of the compounds, and R_2 = *ortho*-Cl is more favored than R_2 = *ortho*-Br (**9b** > **9c**, **6b** > **6o**, and **10b** > **10c**, Fig. 3 and **Table S4** in Supporting Information). Obviously, **9b** and **9c** conferred the most potent neuroprotection among all the tested compounds against the H_2O_2-mediated assaults on PC12 cells.

2.2.2. Relief of PC12 cells from H_2O_2-induced lesions by 9b and 9c

PC12 cells have been demonstrated to possess neuronal characteristics to a great extent and are generally employed as a model for PD studies [39–41,53,55]. Consequently, an injury model based on PC12 cells was engendered to investigate whether **9b** and **9c** could protect the cells from H_2O_2-induced insults. As illustrated in Fig. 4**A** (also shown as values in **Table S5** in Supporting Information), H_2O_2 caused evident death of PC12 cells, and the cell viability treated with H_2O_2 only was about half of the control group. However, when PC12 cells were pretreated with **9b** or **9c**, the H_2O_2-induced cell death was markedly ameliorated at as low concentration as 0.5 μM. Both **9b** and **9c** could elevate the cell viability up to ~ 75% at the concentration of 1 μM. When cells were damaged, the lactate dehydrogenase (LDH) was released from cytoplasm to culture medium on account of the impaired cell membrane

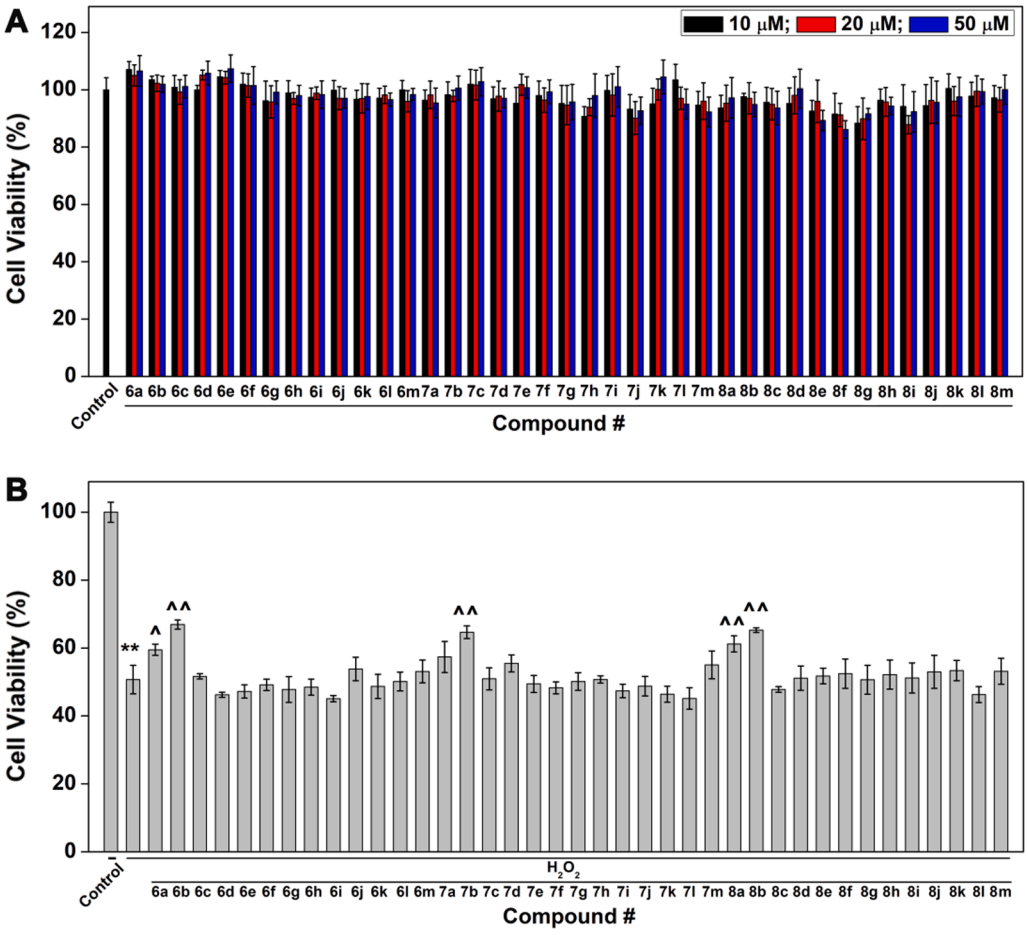

Fig. 1. Cytotoxicity and neuroprotection screening of vinyl sulfone derivatives against PC12 cells. (A) PC12 cells were grown to adhere for 24 h followed by incubation with target compounds (10 μM, 20 μM, and 50 μM) for further 24 h. MTT assay was performed to determine the cell viability. (B) PC12 cells were grown to adhere for 24 h, and then were treated with compounds (1 μM) for another 24 h followed by exposing to the fresh medium containing 500 μM H_2O_2 for further 12 h. Then MTT assay was performed to determine the cell viability. Data are presented as means ± SD from triplicate experiments. $^{**}P < 0.01$ versus the control group; $^{\wedge}P < 0.05$ and $^{\wedge\wedge}P < 0.01$ versus H_2O_2-treated group.

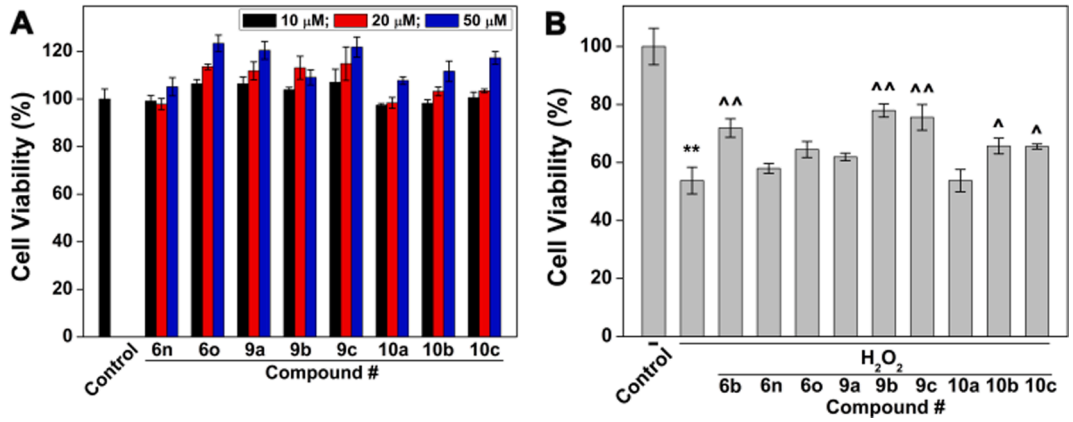

Fig. 2. (A) Cytotoxicity screening of the succedently synthesized vinyl sulfone derivatives against PC12 cells. The experimental details are the same as those described in Fig. 1**A**. (B) Neuroprotection screening of **6b** and the succedently synthesized vinyl sulfone derivatives. The experimental details are the same as those described in Fig. 1**B**. Data are presented as means ± SD from triplicate experiments. $^{**}P < 0.01$ versus the control group; $^{\wedge}P < 0.05$ and $^{\wedge\wedge}P < 0.01$ versus the H_2O_2-treated group.

integrity. Thus a LDH leakage assay was conducted for the purpose of validating the results attained above. As shown in Fig. 4**B**, the content of LDH released in culture medium of solely H_2O_2-treated PC12 cells was two folds more than that of the control group, while pretreatment of PC12 cells with **9b** or **9c** remarkably alleviated the LDH leakage provoked by H_2O_2-mediated damage. Consistently, the LDH leakage assay results were in line with the MTT assay. Taken together, these results pronounced the neuroprotective activity of **9b** and **9c** against H_2O_2-mediated oxidative damages.

2.2.3. *Clearance of ROS in PC12 cells by 9b and 9c treatment*

Oxidative stress-mediated damages to vital cellular components are attributed to the redox imbalance resulting from inadequate antioxidant capacity against the excessive generation of ROS. On this account, we therefore asked if **9b** and **9c** could diminish the ROS production to assuage the oxidative stress-mediated damages inflicted by H_2O_2. Dichlorodihydrofluorescein diacetate (DCFH-DA), a non-fluorescent and cell membrane-permeable probe, was employed to detect ROS. DCFH-DA could easily diffuse into cells and then be hydrolyzed by esterases

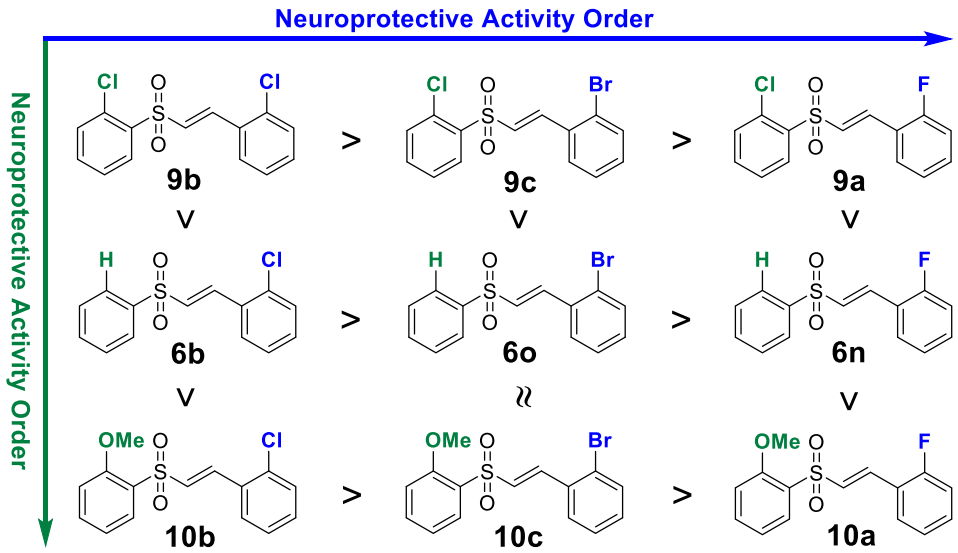

Fig. 3. Structures and neuroprotective activity of the most potent vinyl sulfone derivatives.

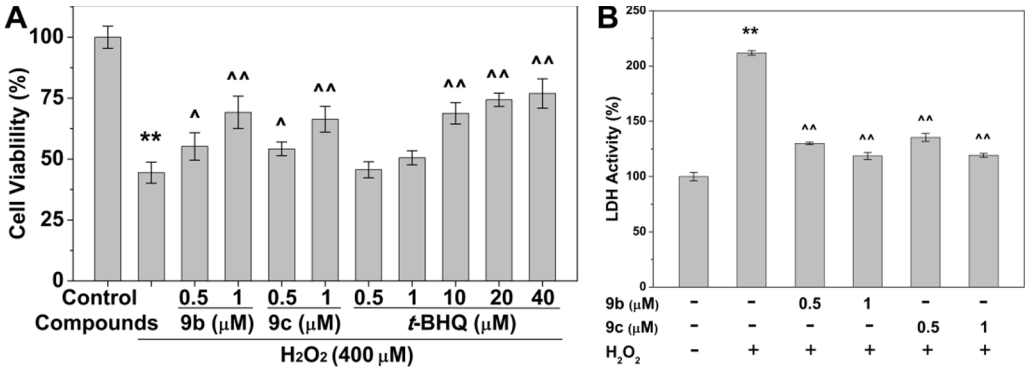

Fig. 4. Neuroprotection of **9b** and **9c** against the H_2O_2-mediated injury to PC12 cells. (A) Dose-dependent protection of **9b** and **9c**. The cells were seeded to adhere for 24 h followed by incubation with **9b** (0.5 μM and 1 μM), **9c** (0.5 μM and 1 μM), and *t*-BHQ (0.5 μM, 1 μM, 10 μM, 20 μM, and 40 μM) for further 24 h, and subsequently the cells were exposed to the fresh medium containing 400 μM H_2O_2 for 12 h. Then MTT assay was performed to determine the cell viability. (B) Validation of the neuroprotection of **9b** and **9c** by measurement of LDH activity in culture medium. The cells were seeded to adhere for 24 h followed by incubation of **9b** (0.5 μM and 1 μM) and **9c** (0.5 μM and 1 μM) for another 24 h, and then were further exposed to fresh medium containing 500 μM H_2O_2 for 12 h. The LDH leakage assay was performed to determine the activity of LDH released in the culture medium. Data are presented as means ± SD from triplicate experiments. $^{**}P < 0.01$ versus the control group; $^{\wedge}P < 0.05$ and $^{\wedge\wedge}P < 0.01$ versus the H_2O_2-treated group.

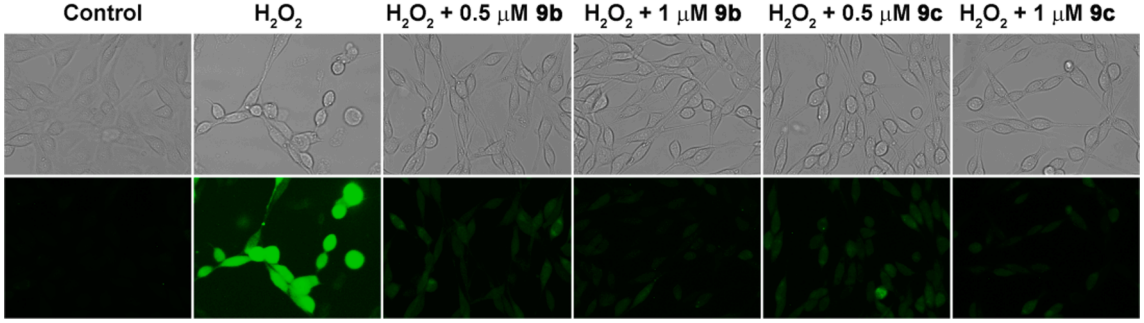

Fig. 5. Mitigation of ROS production by **9b** and **9c** in PC12 cells. The cells were bred to adhere for 24 h, and then were pretreated with **9b** (0.5 μM and 1 μM) and **9c** (0.5 μM and 1 μM) for further 24 h before 500 μM H_2O_2 was added. After the cells were cultured for 5 h, the ROS probe DCFH-DA (10 μM) was loaded. The cells were further cultured for 0.5 h, and the images were taken.

to give non-fluorescent dichlorodihydrofluorescin, which reacts with ROS to afford fluorescent dichlorofluorescein. As depicted in Fig. 5, strong fluorescence was observed in PC12 cells treated with H_2O_2 only, whereas the control group showed marginal fluorescence signal. Prominently, pretreatment of the cells with **9b** or **9c** could significantly alleviate the fluorescence intensity, which indicates that clearance of ROS contributes to the observed neuroprotective effect of **9b** and **9c** (Fig. 4).

2.2.4. Activation of antioxidant response machinery by 9b and 9c in PC12 cells

In consideration of the results that **9b** and **9c** could robustly protect PC12 cells from H_2O_2-induced injuries (Fig. 4), we then speculated that **9b** and **9c** were capable of activation of the cellular antioxidative response machinery via transcriptional activation of cytoprotective genes and up-regulation of corresponding gene products. Afterwards, qRT-PCR was employed to determine several antioxidant/detoxifying genes including *TrxR*, *GCLC* [γ – glutamyl – cysteinyl – ligase (GCL) catalytic subunit], *GCLM* (GCL modulatory subunit), *NQO1*, and *HO-1* after **9b** or **9c** treatment. As displayed in Fig. 6, all these genes were elevated to varying degrees, and elevation of *HO-1* was the most distinct among all the tested genes. **9b** boosted both *NQO1* and *HO-1* at the highest level after 6 h treatment, with 11-fold and 15-fold increase, respectively, and the other three genes remained to be increased and sustainable even at 12 h. Similarly, **9c** promoted *HO-1* at the peak level after 6 h treatment, while the other four genes reached a relatively high level at 12 h. Collectively, these results manifested that **9b** and **9c** efficiently promoted the transcription of the indicated antioxidant/detoxifying genes. Next, we were curious about whether these activated antioxidant/detoxifying genes would be transformed to functional enzymes and molecules, so determination of the content or activity of the corresponding gene products was conducted. GSH, a ubiquitous cellular antioxidant molecule and cardinal thiol-containing tripeptide, is biosynthesized with the aid of GCL that is a heterodimer composed of GCLM and GCLC. As shown in Fig. 7**B**, the content of GSH was promoted to an impressively high level, and the activities of TrxR (Fig. 7**A**), NQO1 (Fig. 7**C**), and HO-1 (Fig. 7**D**) were all elevated to different extents in a dose-dependent manner. In addition, TrxR activity was also confirmed by the TRFS-Green (Fig. 7**E**), which is a fluorescence probe developed by our group [56] to selectively *in situ* detect TrxR activity in live cells. The fluorescence increased accompanied by the elevation of the compounds concentration. Taken together, **9b** and **9c** were capable of efficient activation of cellular antioxidant response system at both transcriptional and translational levels.

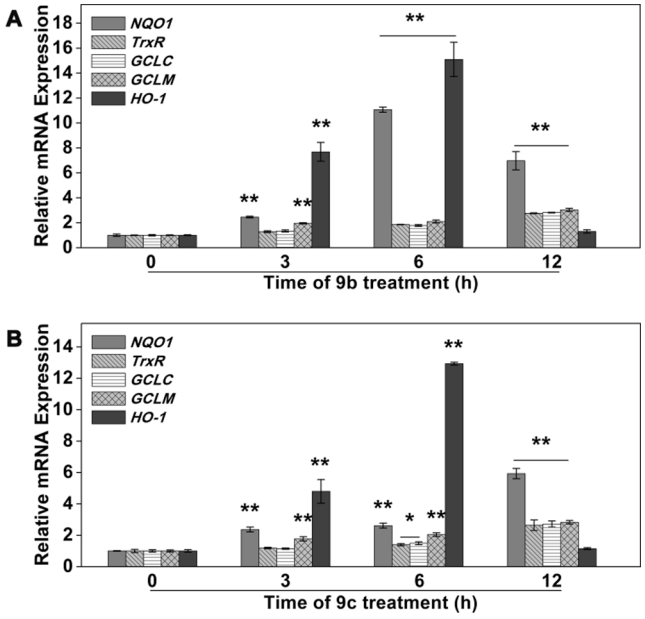

Fig. 6. Transcriptional activation of the antioxidant genes by **9b** and **9c** in PC12 cells. The cells were incubated with **9b** (1 μM) and **9c** (1 μM) for given times, and then the cells were lysed to acquire total RNA. qRT-PCR was employed to analyze the indicated genes expression with GAPDH as a reference. Data are presented as means ± SD from triplicate experiments. $^{*}P < 0.05$ and $^{**}P < 0.01$ versus the control group.

2.2.5. Involvement of Nrf2 for the biological performance of 9b and 9c

Owing to the activation of ARE-directed antioxidant/detoxifying species by **9b** and **9c**, we thereby asked if this phenomenon was Nrf2-dependent. After preparation of cytoplasmic and nuclear fractions of PC12 cells treated with **9b** or **9c**, Western blots analysis was conducted in order to interrogate whether **9b** or **9c** could instigate Nrf2 to migrate from cytoplasm to nucleus, which is indispensable for the antioxidant activity imparted by Nrf2. Although total Nrf2 content was not significantly affected by compounds treatment, cytoplasmic and nuclear Nrf2 level varied gradually (Fig. 8). Consistently, cytoplasmic Nrf2 level declined with concurrent accumulation of nuclear Nrf2, and the coincidental result indicated that Nrf2 translocated from cytoplasm to nucleus. With the intention to confirm the Nrf2-directed initiation of transcription of ARE-dependent cytoprotective genes by **9b** and **9c**, p*ARE*-luciferase plasmid was applied to the transfection of PC12 cells to generate a stable cell line. The classical Nrf2 activator *tert*-butylhydroquinone (*t*-BHQ) was used as a positive control. As shown in Fig. 9**C**, both **9b** and **9c** activated the ARE-luciferase reporter in a dose-dependent manner, and **9b** induced a conspicuously stronger reporter response at such a low concentration as 0.5 μM than *t*-BHQ did at 40 μM. What's more, even **9c** at 1 μM did the similar thing as *t*-BHQ did at 40 μM. Collectively, **9b** and **9c** pronounced as exceedingly sensitive inducers that activated Nrf2-ARE pathway.

To further consolidate the results above, two cell lines were established exploiting short hairpin RNAs (sh*RNA*) to accentuate the necessity of Nrf2 in **9b**- and **9c**-mediated neuroprotection in response to oxidative stress. In specific, sh*NT* (non - targeting plasmid) and sh*Nrf2* (Nrf2 - targeting plasmid) were transfected to PC12 cells to achieve two stable cell lines, and the knockdown efficiency was determined as is shown in Fig. 9**A, B**. Additionally, the knockdown efficiency was also consistently confirmed by the fact that sh*Nrf2* cells were more sensitive to H_2O_2-only treatment than sh*NT* cells (Fig. 9**D**). Therefore the neuroprotection of **9b** and **9c** in the newly generated two cell lines were evaluated (Fig. 9**D** and **Table S6** in **Supporting Information**), and the neuroprotective effects imparted by **9b** and **9c** in PC12 sh*NT* cells were similar as those in the wild type (Fig. 4). However, this effect was drastically abolished in PC12 sh*Nrf2* cells, implying that Nrf2 was definitely implicated in the cytoprotection of **9b** and **9c** against oxidative stress in PC12 cells.

ROS are recognized as both physiologically functional and pathologically detrimental to cells that are endowed with exquisite antioxidant systems to harness ROS for beneficial effects under normal conditions. However, once ROS generation overwhelms the cellular antioxidant response mechanism, oxidative stress ensues. At the same time, the "dark side" of ROS emerges as damaging various cellular components, which results in acceleration of cell senescence and death. Neurodegenerative diseases affect increasing number of people worldwide, while the etiology of the diseases remains controversial. However, mounting evidences discovered in past years indicate that oxidative stress is routinely involved in the etiology of the diseases. Oxidative stress acts as a causal risk factor, or at least an essential auxiliary component, in contributing to the progressive loss of neurons in patients, which is characteristic of neurodegenerative disorders. In this sense, it is tempting to speculate that restoration of redox homeostasis *via* chemotherapeutical intervention might be a promising and feasible strategy to slow or even reverse the progression of the diseases. As a central orchestrator in cellular antioxidant response machinery, Nrf2

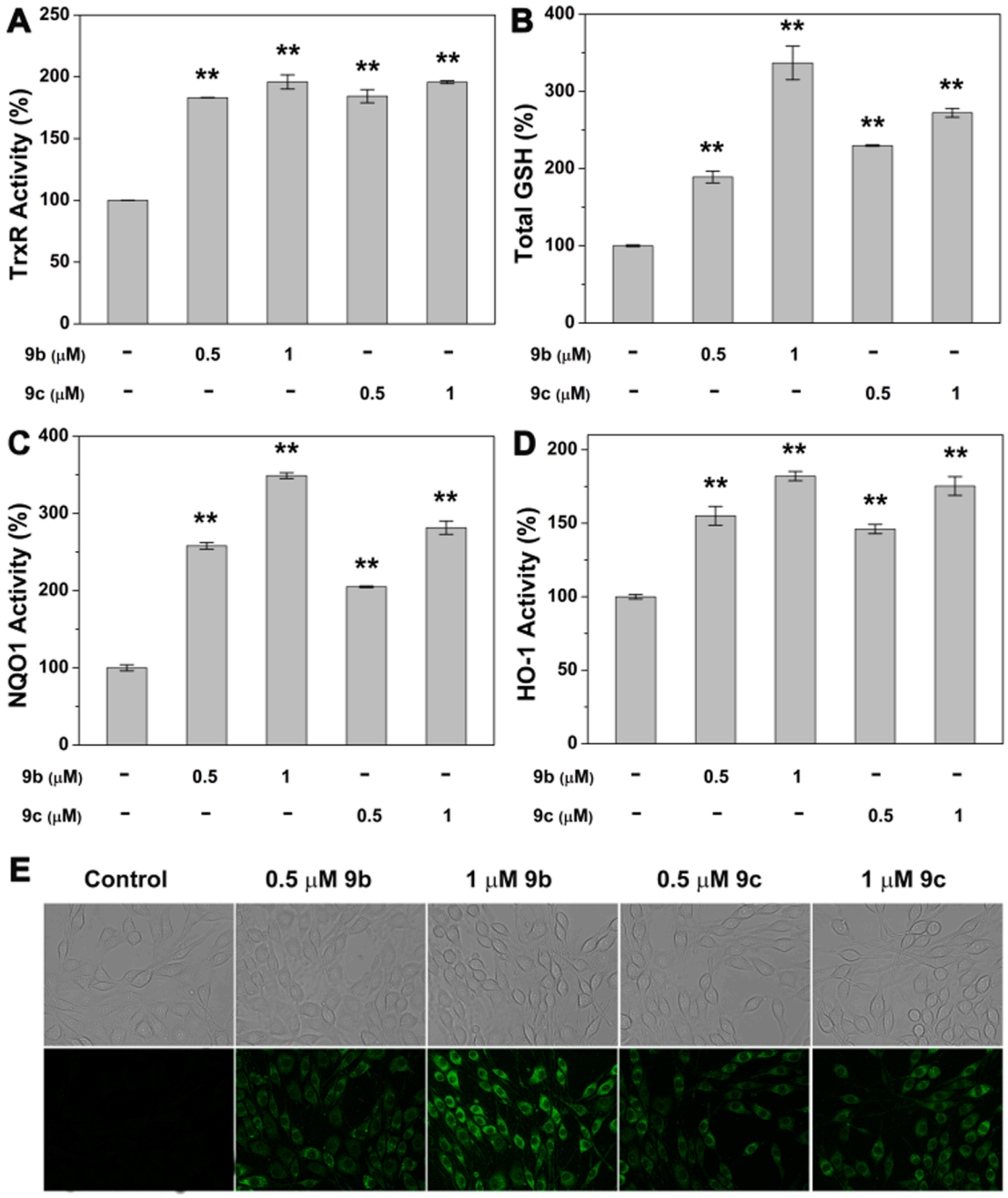

Fig. 7. Elevation of the antioxidant species by **9b** and **9c** in PC12 cells. The cells were seeded to adhere for 24 h followed by incubation of **9b** (0.5 μM and 1 μM) and **9c** (0.5 μM and 1 μM) for further 24 h, and then were lysed to prepare cell samples. Afterwards, the content of GSH (B), and activities of TrxR (A), NQO1 (C), and HO-1 (D) were determined. (E) After incubation of PC12 cells with **9b** (0.5 μM and 1 μM) and **9c** (0.5 μM and 1 μM) for 24 h, TRFS-Green (10 μM) was added for continuous 4 h culture. Then the images were taken. Data are presented as means ± SD from triplicate experiments. $^{**}P < 0.01$ versus the control group. (For interpretation of the references to colour in this figure legend, the reader is referred to the web version of this article.)

emerges as a pharmacological target for neurodegenerative diseases therapeutics.

Chalcones are a family of typical Nrf2 activators according to the classification by Hu *et al.* [18], and the activation property is usually ascribed to their electrophilic double bonds, which could covalently modify the key cysteines in Keap1, eventually leading to the activation of Nrf2. Scaffold of vinyl sulfone, structurally similar to chalcones, is accordingly presumed to have the same properties as chalcones.

As part of our advancing work concerning the identification and development of small redox-regulating molecules targeting Nrf2 activation, we described here the synthesis of vinyl sulfone derivatives and discovered two hit compounds, **9b** and **9c**, with potent neuroprotection against H_2O_2-induced damages. Initial screening, SAR, and optimization studies exhibited herein would be instrumental to further facilitate the optimization and substantiation of this series of compounds. The following studies showed that **9b** and **9c** protected PC12 cells from H_2O_2-mediated insults (Fig. 4) *via* up-regulation of a diverse range of antioxidant species (TrxR, NQO1, GSH, and HO-1) (Fig. 6 and Fig. 7). Mechanistic studies demonstrated that **9b** and **9c** promoted the translocation of Nrf2 (Fig. 8), initiation of Nrf2-dependent activation of ARE (Fig. 9**C**), and finally transcriptional activation of ample antioxidant genes (Fig. 7). Further, silence of Nrf2 in PC12 cells strikingly blunted the neuroprotection (Fig. 9**A, B, and D**), underpinning the indispensable role of Nrf2 in cytoprotection of **9b** and **9c**.

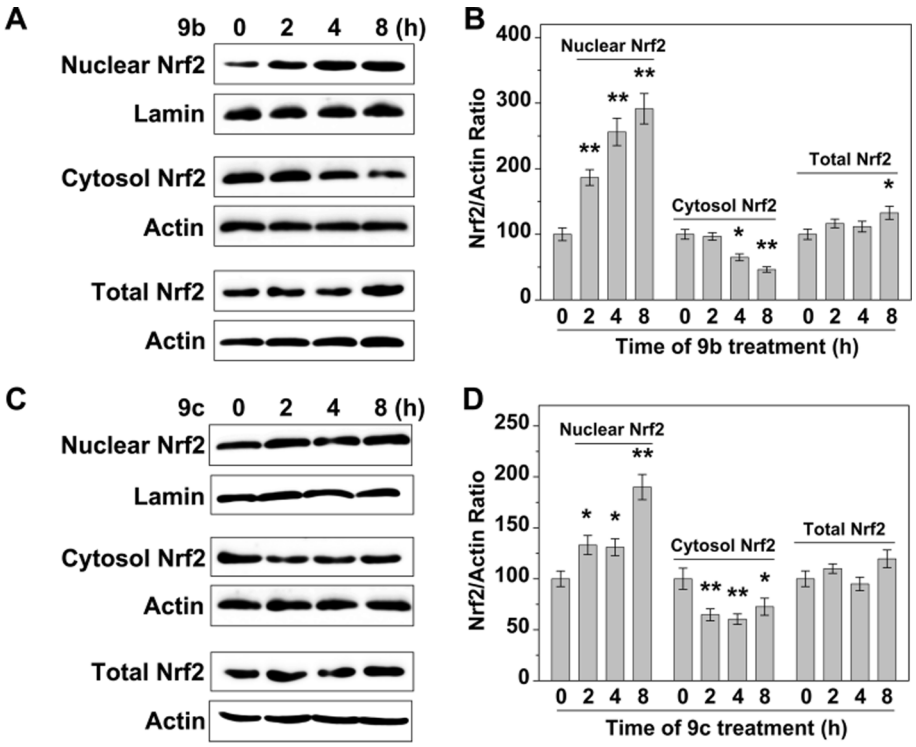

Fig. 8. Variation of Nrf2 location stimulated by **9b** and **9c** in PC12 cells. Incubation of the cells with **9b** (1 μM) and **9c** (1 μM) for different given times, and then the cells were lysed in preparation for different part of protein samples. (A, C) Western blots analysis (WB) of the total, nuclear, and cytosolic Nrf2 after stimulation by **9b** and **9c**. (B, D) Quantification of WB was also expressed. Data are presented as means ± SD from triplicate experiments. *$P < 0.05$ and **$P < 0.01$ versus the control group.

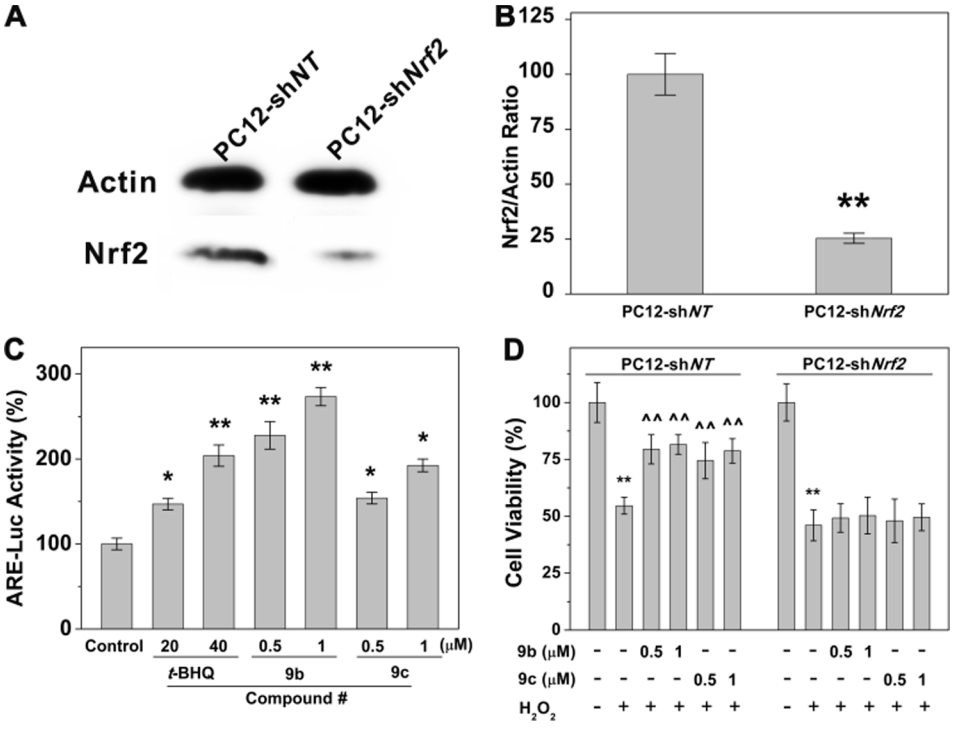

Fig. 9. Essential involvement of Nrf2 in the protection of PC12 cells by **9b** and **9c**. (A) Western blots analysis of Nrf2 expression in PC12-sh*NT* cells and PC12-sh*Nrf2* cells after transfection of PC12 cells with corresponding plasmids. (B) Corresponding quantification result of Western blots analysis. (C) The luciferase reporter gene assay of Nrf2-ARE activation by **9b** and **9c** with *t*-BHQ as a positive control. Transfected PC12 cells were incubated with *t*-BHQ (20 μM and 40 μM), **9b** (0.5 μM and 1 μM), and **9c** (0.5 μM and 1 μM) for 24 h, and then the cells were lysed to prepare samples used for luciferase activity assessment. (D) Neuroprotection of **9b** and **9c** against H_2O_2-induced injuries in PC12-sh*NT* cells and PC12-sh*Nrf2* cells. Data are presented as means ± SD from triplicate experiments. *$P < 0.05$ and **$P < 0.01$ vs vehicle group; ^^$P < 0.01$ vs H_2O_2-treated group.

3. Conclusion

As a whole, 47 vinyl sulfone derivatives were synthesized and evaluated, and two compounds, **9b** and **9c**, were identified to possess the most potent neuroprotective effects. Mechanistic studies showed that **9b** and **9c** activated, promoted the translocation of Nrf2, and thereafter initiated the transcription and expression of a series of antioxidant species. The structural determinants responsible for neuroprotective activity, mechanism of action, and cellular target of **9b** and **9c** were all fully elucidated, which would provide invaluable information for further development of them as potential chemotherapeutical candidates. Further studies to optimize and improve the drug-like properties of them are underway in our lab, and the corresponding *in vivo* experimental results will be reported in due course.

4. Experimental section

4.1. Chemistry

4.1.1. General information

All chemical reagents were purchased from Aladdin (Shanghai, China) without purification, and the reaction solvents were from Kemiou (Tianjin, China). Purification or drying of the reaction solvents is in light of the standard methods. Silica-gel plates (GF254, TLC) and Silica gel (200 ~ 300 mesh) were bought from Qingdao Haiyang (Qingdao, China). ^{1}H NMR (400 MHz) and ^{13}C NMR (100 MHz) spectras of compounds in appropriate solvent were analyzed on a Bruker AMX spectrometer with tetramethylsilane (TMS) as an internal reference. Mass spectra (MS) were recorded on the Shimadzu LCMS-2020 system (ESI-MS).

4.1.2. Purity determination of target compounds by HPLC

Purity analysis of the 47 target compounds were with the assistance of HPLC through the Wondasil C-18 superb reversed-phase column (5 mm, 4.6 mm × 150 mm), which was conducted on the Shimadzu LC-20A system. Water and methanol were both of HPLC grade and employed as the mobile phase. Chromatographically pure methanol was used to dissolve the target compounds that then were injected by 5 μL. The flow rate was 0.6 mL/min, and the detective wavelength ranged from 190 nm to 600 nm to search the maximum absorption wavelength of the tested compounds. The purity of all target compounds is > 95%, which is qualified for the medicinal research. The retention time (t_R) and eluent condition were given for each final compound.

4.1.3. General synthesis of intermediates 3 (3a ~ e) and 4 (4a ~ e)

Intermediates **3** (**3a** ~ **e**) and **4** (**4a** ~ **e**) were synthesized according to the methods described by Park *et al.* [54]. In brief, corresponding thiophenol (**1a** 4.4 g, **1b** 4.97 g, **1c** 5.13 g, **1d** 5.78 g, **1e** 5.61 g, 40 mmol, 1 eq), commercially available intermediate **2** (15.47 g, 48 mmol, 1.2 eq), and Cs_2CO_3 (26.07 g, 80 mmol, 2 eq) were mixed in an appropriate volume (~200 mL) of N, *N*-Dimethylformamide (DMF), the mixture of which was stirred at 70 °C overnight. After concentration of the reaction, the residue was washed with a large amount (~450 mL) of H_2O and extracted with ethyl acetate. The combined organic layer was dried with $MgSO_4$ and evaporated to afford oil materials as corresponding intermediates **3** (**3a** ~ **e**), which were used for next without further purification, and the yields ranged from 85.2% ~ 94.8%. The corresponding oily **3** (**3a** 7.809 g, **3b** 8.229 g, **3c** 8.348 g, **3d** 8.842 g, **3e** 8.709 g, 30 mmol, 1 eq) was dissolved in an appropriate volume (~200 mL) of dichloromethane, and then the reaction was placed in ice. After it was thoroughly cooled, 3-chloroperoxybenzoic acid (*m*-CPBA) (20.708 g, 120 mmol, 4 eq) was added portion-wise. After the addition was completed, it was stirred at room temperature for ~ 5 h and quenched with aqueous $Na_2S_2O_3$ until **3** (**3a** ~ **e**) disappeared. Then it was washed well with aqueous $Na_2S_2O_3$ and water, and extracted with dichloromethane. The combined organic layer was concentrated to give a residue, which was purified on column chromatography to afford pure intermediates **4** (**4a** ~ **e**).

*4.1.3.1. Diethyl ((phenylsulfonyl)methyl)phosphonate (**4a**).* **3a** (7.809 g) and *m*-CPBA (20.708 g) afforded 6.10 g of **4a** as a colorless solid; Yield: 69.6%; mp: 48–49 °C; ^{1}H NMR ($CDCl_3$, 400 MHz) δ: 8.001 (d, 2H, J = 7.6 Hz), 7.681 (t, 1H, J = 7.2 Hz), 7.582 (t, 2H, J = 8 Hz), 4.202–4.126 (m, 4H), 3.826 (d, 2H, J = 16.8 Hz), 1.297 (t, 6H, J = 7.2 Hz); ^{13}C NMR ($CDCl_3$, 100 MHz) δ: 140.018, 134.183, 129.200, 128.395, 63.539, 63.476, 54.501, 53.134, 16.326, 16.262; MS-ESI m/z: 293.05 $[M + H]^+$.

*4.1.3.2. Diethyl (tosylmethyl)phosphonate (**4b**).* **3b** (8.229 g) and *m*-CPBA (20.708 g) afforded 5.72 g of **4b** as a white solid; Yield: 66.2%; mp: 61–62 °C; ^{1}H NMR ($CDCl_3$, 400 MHz) δ: 7.869 (d, 2H, J = 8.4 Hz), 7.364 (d, 2H, J = 8 Hz), 4.200–4.127 (m, 4H), 3.756 (d, 2H, J = 16.8 Hz), 2.448 (s, 3H), 1.299 (t, 6H, J = 7.2 Hz); ^{13}C NMR ($CDCl_3$, 100 MHz) δ: 145.163, 137.086, 129.703, 128.338, 63.366, 63.302, 54.510, 53.145, 21.654, 16.238, 16.175; MS-ESI m/z: 307.05 $[M + H]^+$.

*4.1.3.3. Diethyl (((4-fluorophenyl)sulfonyl)methyl)phosphonate (**4c**).* **3c** (8.348 g) and *m*-CPBA (20.708 g) afforded 6.92 g of **4c** as a white solid; Yield: 74.3%; mp: 74–76 °C; ^{1}H NMR ($CDCl_3$, 400 MHz) δ: 8.061–8.012 m, 2H), 7.283–7.226 (m, 2H), 4.209–4.136 (m, 4H), 3.790 (d, 2H, J = 16.8 Hz), 1.310 (t, 6H, J = 6.8 Hz); ^{13}C NMR ($CDCl_3$, 100 MHz) δ: 167.366, 164.812, 135.926, 135.893, 131.587, 131.490, 130.066, 128.242, 116.540, 116.314, 63.538, 63.474, 54.658, 53.287, 16.309, 16.246; MS-ESI m/z: 311.05 $[M + H]^+$.

*4.1.3.4. Diethyl (((2-chlorophenyl)sulfonyl)methyl)phosphonate (**4d**).* **3d** (8.842 g) and *m*-CPBA (20.708 g) afforded 7.14 g of **4d** as a colorless oil; Yield: 72.8%; mp: colorless oil; ^{1}H NMR ($CDCl_3$, 400 MHz) δ: 8.128 (dd, 1H, J = 1.6 Hz, 8 Hz), 7.588–7.512 (m, 2H), 7.477–7.435 (m, 1H), 4.145–4.038 (m, 6H), 1.244 (t, 6H, J = 6.8 Hz); ^{13}C NMR ($CDCl_3$, 100 MHz) δ: 137.427, 135.148, 132.655, 131.825, 131.795, 127.413, 63.573, 63.508, 52.097, 50.737, 16.256, 16.193; MS-ESI m/z: 327.05 $[M + H]^+$.

*4.1.3.5. Diethyl (((2-methoxyphenyl)sulfonyl)methyl)phosphonate (**4e**).* **3e** (8.709 g) and *m*-CPBA (20.708 g) afforded 6.21 g of **4e** as a colorless solid; Yield: 64.2%; mp: 58–60 °C; ^{1}H NMR ($CDCl_3$, 400 MHz) δ: 7.952 (dd, 1H, J = 1.6 Hz, 7.6 Hz), 7.616–7.573 (m, 1H), 7.097 (t, 1H, J = 7.2 Hz), 7.037 (d, 1H, J = 8.4 Hz), 4.138–4.063 (m, 4H), 4.033 (d, 2H, J = 16.8 Hz), 3.981 (s, 3H), 1.244 (t, 6H, J = 7.2 Hz); ^{13}C NMR ($CDCl_3$, 100 MHz) δ: 157.261, 135.988, 130.397, 127.988, 120.770, 112.368, 63.375, 63.312, 56.525, 52.192, 50.829, 16.307, 16.244; MS-ESI m/z: 323.10 $[M + H]^+$.

4.1.3.6. General synthesis of target compounds (6a ~ o, 7a ~ m, 8a ~ m, 9a ~ c, and 10a ~ c). The synthetic procedure for the target compounds followed the method described by Park *et at.* [54]. Briefly, corresponding intermediate **4** (**4a** 292 mg, **4b** 306 mg, **4c** 310 mg, **4d** 327 mg, **4e** 322 mg, 1 mmol, 1 eq) was dissolved in an appropriate volume (~20 mL) of anhydrous tetrahydrofuran (THF) in schlenk tube, and then it was placed at −78 °C. The tube was degassed three times with argon, and then *n*-BuLi (c = 2 M, 0.6 mL, 1.2 mmol, 1.2 eq) was injected slowly to the reaction at −78 °C. After the reaction was stirred at −78 °C for 1 h, corresponding aldehyde **5** (**5a** ~ **o**) (1.1 mmol, 1.1 eq) diluted in anhydrous THF was injected to the tube at −78 °C, at which temperature the reaction was further stirred for 30 min. Later the reaction was stirred at room temperature for ~ 1 h, which was quenched with saturated aqueous NH_4Cl and extracted with ethyl acetate. The combined organic layer was then concentrated to obtain a residue, which was purified on column chromatography to give the target compound.

*4.1.3.7. (E)-1-(2-(phenylsulfonyl)vinyl)-2-(trifluoromethyl)benzene (**6a**).* **4a** (292 mg, 1 mmol), **5a** (0.15 mL, 1.1 mmol), and *n*-BuLi (c = 2 M, 0.6 mL, 1.2 mmol) gave 286 mg of **6a** as a white solid; Yield: 91.7%; mp: 72–74 °C; ^{1}H NMR ($CDCl_3$, 400 MHz) δ: 8.048 (dq, 1H, J = 15.2 Hz, 2 Hz), 7.973–7.943 (m, 2H), 7.719 (d, 1H, J = 7.6 Hz), 7.668–7.624 (m, 1H), 7.604–7.495 (m, 5H), 6.839 (d, 1H, J = 15.2 Hz); ^{13}C NMR ($CDCl_3$, 100 MHz) δ: 140.032, 138.545, 138.523, 138.501, 138.479, 133.825, 132.402, 131.943, 131.396, 131.378, 130.562, 129.556, 129.362, 129.056, 128.425, 127.977, 126.554, 126.499, 126.445, 126.391, 125.152, 122.428; MS-ESI m/z: 313.05 $[M + H]^+$; Purity: 99.39%, t_R = 5.87 min (20% water in methanol).

*4.1.3.8. (E)-1-chloro-2-(2-(phenylsulfonyl)vinyl)benzene (**6b**).* **4a** (292 mg, 1 mmol), **5b** (0.13 mL, 1.1 mmol), and *n*-BuLi (c = 2 M, 0.6 mL, 1.2 mmol) gave 237 mg of **6b** as a white solid; Yield: 84.9%; mp:

102–103 °C; ^{1}H NMR ($CDCl_3$, 400 MHz) δ: 8.096 (d, 1H, J = 15.6 Hz), 7.985–7.956 (m, 2H), 7.664–7.620 (m, 1H), 7.588–7.547 (m, 2H), 7.514 (dd, 1H, J = 1.6 Hz, 8 Hz), 7.435 (dd, 1H, J = 1.2 Hz, 8 Hz),7.341(td, 1H, J = 1.6 Hz, 8 Hz), 7.285–7.245 (m, 1H), 6.898 (d, 1H, J = 15.6 Hz); ^{13}C NMR ($CDCl_3$, 100 MHz) δ: 140.313, 138.443, 135.383, 133.671, 132.056, 130.688, 130.466, 130.031, 129.501, 128.312, 127.891, 127.322; MS-ESI m/z: 279.00 $[M + H]^+$; Purity: 99.80%, t_R = 6.23 min (20% water in methanol).

4.1.3.9. (E)-1-methoxy-2-(2-(phenylsulfonyl)vinyl)benzene (6c). **4a** (292 mg, 1 mmol), **5c** (0.13 mL, 1.1 mmol), and *n*-BuLi (c = 2 M, 0.6 mL, 1.2 mmol) gave 236 mg of **6c** as a white solid; Yield: 91.8%; mp: 84–85 °C; ^{1}H NMR ($CDCl_3$, 400 MHz) δ: 7.992–7.943 (m, 2H), 7.645–535 (m, 3H), 7.450–7.427 (dd, 1H, J = 1.2 Hz, 8 Hz), 7.301 (td, 1H, J = 1.2 Hz, 7.6 Hz), 7.232–7.167 (m, 2H), 6.784 (d, 1H, J = 15.2 Hz), 2.461 (s, 3H); ^{13}C NMR ($CDCl_3$, 100 MHz) δ: 140.783, 140.219, 138.300, 133.467, 131.322, 131.152, 131.056, 129.446, 128.235, 127.745, 126.957, 126.587, 19.877; MS-ESI m/z: 259.05 $[M + H]^+$; Purity: 99.28%, t_R = 6.03 min (20% water in methanol).

4.1.3.10. (E)-1-methyl-2-(2-(phenylsulfonyl)vinyl)benzene (6d). **4a** (292 mg, 1 mmol), **5d** (150 mg, 1.1 mmol), and *n*-BuLi (c = 2 M, 0.6 mL, 1.2 mmol) gave 259 mg of **6d** as a white solid; Yield: 94.5%; mp: 84–86 °C; ^{1}H NMR ($CDCl_3$, 400 MHz) δ: 7.969–7.940 (m, 2H), 7.894 (d, 1H, J = 15.6 Hz), 7.620–7.512 (m, 3H), 7.427–7.355 (m, 2H), 7.077 (d, 1H, J = 15.6 Hz), 6.978–6.907 (m, 2H), 3.879 (s, 3H); ^{13}C NMR ($CDCl_3$, 100 MHz) δ: 158.893, 141.172, 138.661, 133.219, 132.624, 130.929, 129.319, 127.828, 127.651, 121.164, 120.841, 111.299, 55.581; MS-ESI m/z: 275.05 $[M + H]^+$; Purity: 95.73%, t_R = 5.63 min (20% water in methanol).

4.1.3.11. (E)-1-(2-(phenylsulfonyl)vinyl)-3-(trifluoromethyl)benzene (6e). **4a** (292 mg, 1 mmol), **5e** (192 mg, 1.1 mmol), and *n*-BuLi (c = 2 M, 0.6 mL, 1.2 mmol) gave 279 mg of **6e** as a white solid; Yield: 89.4%; mp: 90–92 °C; ^{1}H NMR ($CDCl_3$, 400 MHz) δ: 7.958–7.936 (m, 2H), 7.708–7.591 (m, 5H), 7.552–7.480 (m, 3H), 6.995 (d, 1H, J = 15.6 Hz); ^{13}C NMR ($CDCl_3$, 100 MHz) δ: 140.531, 140.131, 133.710, 133.148, 131.772, 131.630, 131.305, 130.975, 129.757, 129.474, 129.439, 128.831, 127.764, 127.567, 127.531, 127.493, 127.456, 125.093, 125.055, 125.017, 124.979, 124.951; MS-ESI m/z: 313.05 $[M + H]^+$; Purity: 96.90%, t_R = 6.09 min (20% water in methanol).

4.1.3.12. (E)-1-chloro-3-(2-(phenylsulfonyl)vinyl)benzene (6f). **4a** (292 mg, 1 mmol), **5f** (0.13 mL, 1.1 mmol), and *n*-BuLi (c = 2 M, 0.6 mL, 1.2 mmol) gave 238 mg of **6f** as a white solid; Yield: 85.3%; mp: 92–94 °C; ^{1}H NMR ($CDCl_3$, 400 MHz) δ: 7.958–7.935 (m, 2H), 7.660–7.546 (m, 4H), 7.469 (s, 1H), 7.401–7.260 (m, 3H), 6.872 (d, 1H, J = 15.2 Hz); ^{13}C NMR ($CDCl_3$, 100 MHz) δ: 140.831, 140.381, 135.209, 134.214, 133.709, 131.159, 130.454, 129.530, 128.959, 128.284, 127.844, 126.935; MS-ESI m/z: 279.00 $[M + H]^+$; Purity: 97.98%, t_R = 6.23 min (20% water in methanol).

4.1.3.13. (E)-1-methoxy-3-(2-(phenylsulfonyl)vinyl)benzene (6 g). **4a** (292 mg, 1 mmol), **5 g** (0.13 mL, 1.1 mmol), and *n*-BuLi (c = 2 M, 0.6 mL, 1.2 mmol) gave 237 mg of **6 g** as a colorless solid; Yield: 91.9%; mp: 71–73 °C; ^{1}H NMR ($CDCl_3$, 400 MHz) δ: 7.963–7.933 (m, 2H), 7.660 (d, 1H, J = 15.6 Hz), 7.634–7.594 (m, 1H), 7.564–7.524 (m, 2H), 7.379 (d, 2H, J = 8.4 Hz), 7.194 (d, 2H, J = 8.4 Hz), 6.805 (d, 1H, J = 15.6 Hz), 2.368 (s, 3H); ^{13}C NMR ($CDCl_3$, 100 MHz) δ: 142.827, 140.910, 138.980, 133.465, 132.411, 132.193, 129.448, 129.273, 129.098, 127.762, 127.100, 125.963, 21.406; MS-ESI m/z: 259.05 $[M + H]^+$; Purity: 98.38%, t_R = 6.18 min (20% water in methanol).

4.1.3.14. (E)-1-methyl-3-(2-(phenylsulfonyl)vinyl)benzene (6 h). **4a** (292 mg, 1 mmol), **5 h** (150 mg, 1.1 mmol), and *n*-BuLi (c = 2 M, 0.6 mL, 1.2 mmol) gave 260 mg of **6 h** as a white solid; Yield: 94.7%; mp: 101–103 °C; ^{1}H NMR ($CDCl_3$, 400 MHz) δ: 7.959–7.938 (m, 2H), 7.672–7.602 (m, 2H), 7.570–7.530 (m, 2H), 7.301 (t, 1H, J = 8 Hz), 7.075 (d, 1H, J = 7.6 Hz), 6.990–6.931 (m, 2H), 6.850 (d, 1H, J = 15.6 Hz), 3.809 (s, 3H); ^{13}C NMR ($CDCl_3$, 100 MHz) δ: 160.065, 142.545, 140.760, 133.742, 133.511, 130.209, 129.450, 127.759, 127.625, 121.319, 117.238, 113.472, 55.464; MS-ESI m/z: 275.05 $[M + H]^+$; Purity: 98.55%, t_R = 5.48 min (20% water in methanol).

4.1.3.15. (E)-1-(2-(phenylsulfonyl)vinyl)-4-(trifluoromethyl)benzene (6i). **4a** (292 mg, 1 mmol), **5i** (0.16 mL, 1.1 mmol), and *n*-BuLi (c = 2 M, 0.6 mL, 1.2 mmol) gave 280 mg of **6i** as a white solid; Yield: 89.8%; mp: 127–129 °C; ^{1}H NMR ($CDCl_3$, 400 MHz) δ: 7.971–7.949 (m, 2H), 7.708 (d, 1H, J = 15.6 Hz), 7.664–7.634 (m, 3H), 7.605–7.555 (m, 4H), 6.955 (d, 1H, J = 15.6 Hz); ^{13}C NMR ($CDCl_3$, 100 MHz) δ: 140.551, 140.206, 135.847, 135.832, 133.845, 132.882, 132.554, 130.113, 129.595, 128.872, 127.929, 126.223, 126.185, 126.147, 126.109, 125.056, 122.349; MS-ESI m/z: 313.15 $[M + H]^+$; Purity: 98.05%, t_R = 5.78 min (20% water in methanol).

4.1.3.16. (E)-1-chloro-4-(2-(phenylsulfonyl)vinyl)benzene (6j). **4a** (292 mg, 1 mmol), **5j** (155 mg, 1.1 mmol), and *n*-BuLi (c = 2 M, 0.6 mL, 1.2 mmol) gave 238 mg of **6j** as a white solid; Yield: 85.6%; mp: 125–126 °C; ^{1}H NMR ($CDCl_3$, 400 MHz) δ: 7.958–7.936 (m, 2H), 7.657–7.542 (m, 4H), 7.394 (dd, 4H, J = 8.4 Hz, 20.8 Hz), 6.838 (d, 1H, J = 15.6 Hz); ^{13}C NMR ($CDCl_3$, 100 MHz) δ: 141.020, 140.432, 137.236, 133.600, 130.839, 129.829, 129.457, 129.413, 127.871, 127.719; MS-ESI m/z: 279.00 $[M + H]^+$; Purity: 99.49%, t_R = 5.82 min (20% water in methanol).

4.1.3.17. (E)-1-methoxy-4-(2-(phenylsulfonyl)vinyl)benzene (6 k). **4a** (292 mg, 1 mmol), **5 k** (0.13 mL, 1.1 mmol), and *n*-BuLi (c = 2 M, 0.6 mL, 1.2 mmol) gave 247 mg of **6 k** as a white solid; Yield: 95.8%; mp: 130–132 °C; ^{1}H NMR ($CDCl_3$, 400 MHz) δ: 7.956–7.934 (m, 2H), 7.678–7.523 (m, 4H), 7.379 (d, 2H, J = 8 Hz), 7.194 (d, 2H, J = 8 Hz), 6.804 (d, 1H, J = 15.2 Hz), 2.370 (s, 3H); ^{13}C NMR ($CDCl_3$, 100 MHz) δ: 142.658, 141.973, 141.013, 133.377, 129.908, 129.695, 129.400, 128.693, 127.680, 126.142, 21.634; MS-ESI m/z: 259.05 $[M + H]^+$; Purity: 98.54%, t_R = 6.00 min (20% water in methanol).

4.1.3.18. (E)-1-methyl-4-(2-(phenylsulfonyl)vinyl)benzene (6 l). **4a** (292 mg, 1 mmol), **5 l** (0.14 mL, 1.1 mmol), and *n*-BuLi (c = 2 M, 0.6 mL, 1.2 mmol) gave 258 mg of **6 l** as a white solid; Yield: 94.2%; mp: 113–115 °C; ^{1}H NMR ($CDCl_3$, 400 MHz) δ: 7.942 (d, 2H, J = 7.6 Hz), 7.654–7.518 (m, 4H), 7.434 (d, 2H, J = 7.6 Hz), 6.897 (d, 2H, J = 8.8 Hz), 6.709 (d, 1H, J = 15.6 Hz), 3.831 (s, 3H); ^{13}C NMR ($CDCl_3$, 100 MHz) δ: 162.156, 142.377, 141.222, 133.261, 130.476, 129.357, 127.575, 125.026, 124.497, 114.600, 55.532; MS-ESI m/z: 275.05 $[M + H]^+$; Purity: 97.44%, t_R = 5.23 min (20% water in methanol).

4.1.3.19. (E)-(2-(phenylsulfonyl)vinyl)benzene (6 m). **4a** (292 mg, 1 mmol), **5 m** (0.12 mL, 1.1 mmol), and *n*-BuLi (c = 2 M, 0.6 mL, 1.2 mmol) gave 237 mg of **6 m** as a colorless solid; Yield: 97.1%; mp: 72–74 °C; ^{1}H NMR ($CDCl_3$, 400 MHz) δ: 7.971–7.942 (m, 2H), 7.694 (d, 1H, J = 15.2 Hz), 7.648–7.605 (m, 1H), 7.573–7.533 (m, 2H), 7.508–7.477 (m, 2H), 7.442–7.368 (m, 3H), 6.865 (d, 1H, J = 15.6 Hz), ^{13}C NMR ($CDCl_3$, 100 MHz) δ: 142.470, 140.633, 133.425, 132.262, 131.241, 129.357, 129.078, 128.585, 127.609, 127.223; MS-ESI m/z: 245.05 $[M + H]^+$; Purity: 98.89%, t_R = 5.08 min (20% water in methanol).

4.1.3.20. (E)-1-bromo-2-(2-(phenylsulfonyl)vinyl)benzene (6n). **4a** (292 mg, 1 mmol), **5n** (0.12 mL, 1.1 mmol), and *n*-BuLi (c = 2 M, 0.6 mL, 1.2 mmol) gave 246 mg of **6n** as a colorless solid; Yield: 93.9%; mp: 72–73 °C; ^{1}H NMR ($CDCl_3$, 400 MHz) δ: 7.960 (d, 2H, J = 7.6 Hz), 7.769

(d, 1H, J = 15.6 Hz), 7.650–7.541 (m, 3H), 7.486–7.369 (m, 2H), 7.194–7.074 (m, 2H), 7.024 (d, 1H, J = 15.6 Hz); ^{13}C NMR ($CDCl_3$, 100 MHz) δ: 162.869, 160.332, 140.562, 135.580, 135.557, 133.575, 132.909, 132.821, 130.381, 130.355, 130.281, 130.197, 129.461, 127.817, 124.802, 124.765, 120.668, 120.555, 116.575, 116.359; MS-ESI m/z: 263.05 $[M + H]^+$; Purity: 99.65%, t_R = 5.50 min (20% water in methanol).

*4.1.3.21. (E)-1-fluoro-2-(2-(phenylsulfonyl)vinyl)benzene (**6o**).* **4a** (292 mg, 1 mmol), **5o** (0.13 mL, 1.1 mmol), and *n*-BuLi (c = 2 M, 0.6 mL, 1.2 mmol) gave 305 mg of **6o** as a colorless solid; Yield: 94.8%; mp: 89–90 °C; ^{1}H NMR ($CDCl_3$, 400 MHz) δ: 8.061 (d, 1H, J = 15.6 Hz), 7.992–7.962 (m, 2H), 7.662–7.547 (m, 4H), 7.496 (dd, 1H, J = 2 Hz, 7.6 Hz), 7.311 (td, 1H, J = 1.2 Hz, 7.6 Hz), 7.272–7.230 (m, 1H), 6.846 (d, 1H, J = 15.2 Hz); ^{13}C NMR ($CDCl_3$, 100 MHz) δ: 140.968, 140.289, 133.639, 133.570, 132.537, 132.053, 130.248, 129.415, 128.271, 127.853, 125.574; MS-ESI m/z: 322.95 $[M + H]^+$; Purity: 99.36%, t_R = 6.49 min (20% water in methanol).

*4.1.3.22. (E)-1-(2-tosylvinyl)-2-(trifluoromethyl)benzene (**7a**).* **4b** (306 mg, 1 mmol), **5a** (0.15 mL, 1.1 mmol), and *n*-BuLi (c = 2 M, 0.6 mL, 1.2 mmol) gave 289 mg of **7a** as a white solid; Yield: 88.7%; mp: 106–107 °C; ^{1}H NMR ($CDCl_3$, 400 MHz) δ: 8.013 (dd, 1H, J = 2.4 Hz, 15.2 Hz), 7.830 (d, 2H, J = 8.4 Hz), 7.710 (d, 1H, J = 7.6 Hz), 7.591–7.484 (m, 3H), 7.358 (d, 2H, J = 8 Hz), 6.821 (d, 1H, J = 14.8 Hz), 2.441 (s, 3H); ^{13}C NMR ($CDCl_3$, 100 MHz) δ: 144.891, 137.927, 137.905, 137.076, 132.376, 132.291, 131.489, 130.441, 130.167, 129.292, 128.987, 128.389, 128.006, 126.503, 126.449, 126.394, 126.340, 125.166, 122.442, 21.733; MS-ESI m/z: 327.00 $[M + H]^+$; Purity: 99.87%, t_R = 6.90 min (20% water in methanol).

*4.1.3.23. (E)-1-chloro-2-(2-tosylvinyl)benzene (**7b**).* **4b** (306 mg, 1 mmol), **5b** (0.13 mL, 1.1 mmol), and *n*-BuLi (c = 2 M, 0.6 mL, 1.2 mmol) gave 243 mg of **7b** as a white solid; Yield: 83.1%; mp: 104–105 °C; ^{1}H NMR ($CDCl_3$, 400 MHz) δ: 8.057 (d, 1H, J = 15.6 Hz), 7.842 (d, 2H, J = 8 Hz), 7.500 (dd, 1H, J = 2 Hz, 7.6 Hz), 7.427 (dd, 1H, J = 1.2 Hz, 8 Hz), 7.366–7.308 (m, 3H), 7.276–7.239 (m, 1H), 2.442 (s, 3H); ^{13}C NMR ($CDCl_3$, 100 MHz) δ: 144.714, 137.930, 137.397, 135.351, 131.934, 130.846, 130.461, 130.441, 130.137, 128.295, 127.972, 127.303, 21.759; MS-ESI m/z: 293.00 $[M + H]^+$; Purity: 99.86%, t_R = 7.36 min (20% water in methanol).

*4.1.3.24. (E)-1-methoxy-2-(2-tosylvinyl)benzene (**7c**).* **4b** (306 mg, 1 mmol), **5c** (0.13 mL, 1.1 mmol), and *n*-BuLi (c = 2 M, 0.6 mL, 1.2 mmol) gave 253 mg of **7c** as a white solid; Yield: 92.9%; mp: 81–83 °C; ^{1}H NMR ($CDCl_3$, 400 MHz) δ: 7.940 (d, 1H, J = 15.2 Hz), 7.829 (d, 2H, J = 8.4 Hz), 7.426 (d, 1H, J = 7.6 Hz), 7.347 (d, 2H, J = 8 Hz), 7.293 (t, 1H, J = 6.8 Hz), 7.223–7.163 (m, 2H), 6.767 (d, 1H, J = 15.2 Hz), 2.453 (s, 3H), 2.440 (s, 3H); ^{13}C NMR ($CDCl_3$, 100 MHz) δ: 144.448, 139.656, 138.213, 137.794, 131.403, 131.106, 130.925, 130.064, 128.570, 127.788, 126.907, 126.548, 21.724, 19.872; MS-ESI m/z: 273.05 $[M + H]^+$; Purity: 98.98%, t_R = 7.16 min (20% water in methanol).

*4.1.3.25. (E)-1-methyl-2-(2-tosylvinyl)benzene (**7d**).* **4b** (306 mg, 1 mmol), **5d** (150 mg, 1.1 mmol), and *n*-BuLi (c = 2 M, 0.6 mL, 1.2 mmol) gave 261 mg of **7d** as a white solid; Yield: 90.4%; mp: 70–73 °C; ^{1}H NMR ($CDCl_3$, 400 MHz) δ: 7.882–7.815 (m, 3H), 7.416–7.316 (m, 4H), 7.065 (d, 1H, J = 15.6 Hz), 6.970–6.899 (m, 2H), 3.870 (s, 3H), 2.423 (s, 3H); ^{13}C NMR ($CDCl_3$, 100 MHz) δ: 158.770, 144.102, 138.128, 138.020, 132.462, 130.765, 129.894, 128.101, 127.624, 121.138, 120.750, 111.220, 55.500, 21.643; MS-ESI m/z: 289.05 $[M + H]^+$; Purity: 96.75%, t_R = 6.64 min (20% water in methanol).

*4.1.3.26. (E)-1-(2-tosylvinyl)-3-(trifluoromethyl)benzene (**7e**).* **4b** (306 mg, 1 mmol), **5e** (192 mg, 1.1 mmol), and *n*-BuLi (c = 2 M, 0.6 mL, 1.2 mmol) gave 288 mg of **7e** as a white solid; Yield: 88.4%; mp: 96–98 °C; ^{1}H NMR ($CDCl_3$, 400 MHz) δ: 7.835 (d, 2H, J = 8.4 Hz), 7.714–7.643 (m, 4H), 7.539 (d, 1H, J = 7.6 Hz), 7.361 (d, 2H, J = 8 Hz), 6.931 (d, 1H, J = 15.6 Hz), 2.444 (s, 3H); ^{13}C NMR ($CDCl_3$, 100 MHz) δ: 144.920, 141.943, 140.075, 137.296, 133.412, 131.928, 131.768, 131.600, 130.225, 129.922, 129.817, 129.048, 127.987, 127.583, 127.545, 125.099, 125.059, 21.768; MS-ESI m/z: 327.00 $[M + H]^+$; Purity: 97.53%, t_R = 7.22 min (20% water in methanol).

*4.1.3.27. (E)-1-chloro-3-(2-tosylvinyl)benzene (**7f**).* **4b** (306 mg, 1 mmol), **5f** (0.13 mL, 1.1 mmol), and *n*-BuLi (c = 2 M, 0.6 mL, 1.2 mmol) gave 239 mg of **7f** as a white solid; Yield: 81.8%; mp: 91–93 °C; ^{1}H NMR ($CDCl_3$, 400 MHz) δ: 7.821 (d, 2H, J = 8 Hz), 7.586 (d, 1H, J = 15.6 Hz), 7.454 (s, 1H), 7.390–7.303 (m, 5H), 6.856 (d, 1H, J = 15.2 Hz), 2.442 (s, 3H); ^{13}C NMR ($CDCl_3$, 100 MHz) δ: 144.766, 140.265, 137.424, 135.188, 134.342, 131.036, 130.426, 130.158, 129.334, 128.239, 127.907, 126.860, 21.753; MS-ESI m/z: 293.00 $[M + H]^+$; Purity: 98.77%, t_R = 7.40 min (20% water in methanol).

*4.1.3.28. (E)-1-methoxy-3-(2-tosylvinyl)benzene (**7 g**).* **4b** (306 mg, 1 mmol), **5 g** (0.13 mL, 1.1 mmol), and *n*-BuLi (c = 2 M, 0.6 mL, 1.2 mmol) gave 246 mg of **7 g** as a white solid; Yield: 90.4%; mp: 93–94 °C; ^{1}H NMR ($CDCl_3$, 400 MHz) δ: 7.824 (d, 2H, J = 7.6 Hz), 7.627 (d, 1H, J = 15.6 Hz), 7.337 (d, 2H, J = 8 Hz), 7.280–7.261 (m, 3H), 7.247–7.205 (m, 1H), 6.831 (m, 1H, J = 15.2 Hz), 2.431 (s, 3H), 2.347 (s, 3H); ^{13}C NMR ($CDCl_3$, 100 MHz) δ: 144.415, 142.206, 138.887, 137.917, 132.471, 132.025, 130.037, 129.180, 129.027, 127.772, 127.442, 125.856, 21.714, 21.360; MS-ESI m/z: 273.05 $[M + H]^+$; Purity: 99.56%, t_R = 7.37 min (20% water in methanol).

*4.1.3.29. (E)-1-methyl-3-(2-tosylvinyl)benzene (**7 h**).* **4b** (306 mg, 1 mmol), **5 h** (150 mg, 1.1 mmol), and *n*-BuLi (c = 2 M, 0.6 mL, 1.2 mmol) gave 270 mg of **7 h** as a colorless solid; Yield: 93.8%; mp: 56–58 °C; ^{1}H NMR ($CDCl_3$, 400 MHz) δ: 7.820 (d, 2H, J = 8.4 Hz), 7.626 (d, 1H, J = 15.6 Hz), 7.358–7.266 (m, 3H), 7.069 (d, 1H, J = 7.6 Hz), 6.977–6.940 (m, 2H), 6.840 (d, 1H, J = 15.2 Hz), 3.810 (s, 3H), 2.438 (s, 3H); ^{13}C NMR ($CDCl_3$, 100 MHz) δ: 159.701, 144.237, 141.657, 137.488, 133.494, 129.885, 129.812, 127.710, 127.473, 121.025, 116.876, 113.058, 55.138, 21.415; MS-ESI m/z: 289.05 $[M + H]^+$; Purity: 98.93%, t_R = 6.42 min (20% water in methanol).

*4.1.3.30. (E)-1-chloro-4-(2-tosylvinyl)benzene (**7i**).* **4b** (306 mg, 1 mmol), **5i** (0.16 mL, 1.1 mmol), and *n*-BuLi (c = 2 M, 0.6 mL, 1.2 mmol) gave 301 mg of **7i** as a white solid; Yield: 92.4%; mp: 127–128 °C; ^{1}H NMR ($CDCl_3$, 400 MHz) δ: 7.835 (d, 2H, J = 8.4 Hz), 7.691–7.571 (m, 5H), 7.363 (d, 2H, J = 8 Hz), 7.940 (d, 1H, J = 15.6 Hz), 2.445 (s, 3H); ^{13}C NMR ($CDCl_3$, 100 MHz) δ: 144.955, 139.985, 137.137, 135.910, 130.362, 130.218, 128.806, 127.968, 126.174, 126.138, 126.100, 126.062, 21.772; MS-ESI m/z: 327.05 $[M + H]^+$; Purity: 99.49%, t_R = 6.74 min (20% water in methanol).

*4.1.3.31. (E)-1-methoxy-4-(2-tosylvinyl)benzene (**7j**).* **4b** (306 mg, 1 mmol), **5j** (155 mg, 1.1 mmol), and *n*-BuLi (c = 2 M, 0.6 mL, 1.2 mmol) gave 248 mg of **7j** as a white solid; Yield: 84.8%; mp: 140–142 °C; ^{1}H NMR ($CDCl_3$, 400 MHz) δ: 7.820 (d, 2H, J = 8.4 Hz), 7.603 (d, 1H, J = 15.6 Hz), 7.417–7.340 (m, 6H), 6.822 (d, 1H, J = 15.2 Hz), 2.439 (s, 3H); ^{13}C NMR ($CDCl_3$, 100 MHz) δ: 144.668, 140.490, 137.458, 137.149, 130.955, 130.112, 129.784, 129.420, 128.212, 127.811, 21.738; MS-ESI m/z: 293.00 $[M + H]^+$; Purity: 95.03%, t_R = 6.55 min (20% water in methanol).

*4.1.3.32. (E)-1-methyl-4-((4-(trifluoromethyl)styryl)sulfonyl)benzene (**7 k**).* **4b** (306 mg, 1 mmol), **5 k** (0.13 mL, 1.1 mmol), and *n*-BuLi (c = 2 M, 0.6 mL, 1.2 mmol) gave 262 mg of **7 k** as a white solid; Yield: 96.4%; mp: 148–150 °C; ^{1}H NMR ($CDCl_3$, 400 MHz) δ: 7.821 (d, 2H, J = 8.4 Hz),

7.625 (d, 1H, J = 15.2 Hz), 7.376–7.325 (m, 4H), 7.186 (d, 2H, J = 8 Hz), 6.788 (d, 1H, J = 15.2 Hz), 2.431 (s, 3H), 2.366 (s, 3H); ^{13}C NMR ($CDCl_3$, 100 MHz) δ: 144.343, 142.083, 141.805, 138.033, 130.017, 129.867, 129.774, 128.619, 127.727, 126.488, 21.701, 21.608; MS-ESI m/z: 273.05 $[M + H]^+$; Purity: 98.95%, t_R = 7.12 min (20% water in methanol).

*4.1.3.33. (E)-1-methyl-4-((4-methylstyryl)sulfonyl)benzene (**7 l**).* **4b** (306 mg, 1 mmol), **5 l** (0.14 mL, 1.1 mmol), and *n*-BuLi (c = 2 M, 0.6 mL, 1.2 mmol) gave 275 mg of **7 l** as a white solid; Yield: 95.6%; mp: 92–93 °C; ^{1}H NMR ($CDCl_3$, 400 MHz) δ: 7.816 (d, 2H, J = 8 Hz), 7.602 (d, 1H, J = 15.2 Hz), 7.421 (d, 2H, J = 8.8 Hz), 7.330 (d, 2H, J = 7.6 Hz), 6.891 (d, 2H, J = 8.8 Hz), 6.694 (d, 1H, J = 15.6 Hz), 3.829 (s, 3H), 2.427 (s, 3H); ^{13}C NMR ($CDCl_3$, 100 MHz) δ: 162.060, 144.227, 141.826, 138.259, 130.406, 129.995, 127.652, 125.131, 124.877, 114.575, 55.535, 21.708; MS-ESI m/z: 289.05 $[M + H]^+$; Purity: 99.08%, t_R = 6.12 min (20% water in methanol).

*4.1.3.34. (E)-1-fluoro-4-(styrylsulfonyl)benzene (**7 m**).* **4b** (306 mg, 1 mmol), **5 m** (0.12 mL, 1.1 mmol), and *n*-BuLi (c = 2 M, 0.6 mL, 1.2 mmol) gave 247 mg of **7 m** as a colorless solid; Yield: 95.6%; mp: 118–119 °C; ^{1}H NMR ($CDCl_3$, 400 MHz) δ: 7.830 (d, 2H, J = 8.4 Hz), 7.659 (d, 1H, J = 15.6 Hz), 7.488–7.464 (m, 2H), 7.414–7.333 (m, 5H), 7.848 (d, 1H, J = 15.6 Hz), 2.435 (s, 3H); ^{13}C NMR ($CDCl_3$, 100 MHz) δ: 144.493, 142.025, 137.830, 132.536, 131.204, 130.070, 129.158, 128.619, 127.805, 127.717, 21.724; MS-ESI m/z: 259.10 $[M + H]^+$; Purity: 99.12%, t_R = 5.88 min (20% water in methanol).

*4.1.3.35. (E)-1-(2-((4-fluorophenyl)sulfonyl)vinyl)-2-(trifluoromethyl) benzene (**8a**).* **4c** (310 mg, 1 mmol), **5a** (0.15 mL, 1.1 mmol), and *n*-BuLi (c = 2 M, 0.6 mL, 1.2 mmol) gave 294 mg of **8a** as a white solid; Yield: 89.1%; mp: 82–83 °C; ^{1}H NMR ($CDCl_3$, 400 MHz) δ: 8.060 (dq, 1H, J = 2 Hz, 15.2 Hz), 8.010–7.960 (m, 2H), 7.743 (d, 1H, J = 7.6 Hz), 7.626–7.524 (m, 3H), 7.289–7.232 (m, 2H), 6.836 (d, 1H, J = 15.2 Hz); ^{13}C NMR ($CDCl_3$, 100 MHz) δ: 167.202, 164.652, 138.759, 138.738, 138.716, 136.214, 136.182, 132.445, 131.871, 131.310, 131.294, 130.930, 130.834, 130.657, 129.705, 129.399, 129.094, 128.788, 128.441, 127.889, 126.607, 126.552, 126.497, 126.442, 125.165, 122.441, 117.009, 116.784; MS-ESI m/z: 331.00 $[M + H]^+$; Purity: 99.60%, t_R = 6.27 min (20% water in methanol).

*4.1.3.36. (E)-1-(2-((4-fluorophenyl)sulfonyl)vinyl)-2-methoxybenzene (**8b**).* **4c** (310 mg, 1 mmol), **5b** (0.13 mL, 1.1 mmol), and *n*-BuLi (c = 2 M, 0.6 mL, 1.2 mmol) gave 247 mg of **8b** as a white solid; Yield: 83.4%; mp: 104–105 °C; ^{1}H NMR ($CDCl_3$, 400 MHz) δ: 8.082 (d, 1H, J = 15.6 Hz), 8.006–7.957 (m, 2H), 7.512 (dd, 1H, J = 1.6 Hz, 7.6 Hz), 7.441 (dd, 1H, J = 1.2 Hz, 8 Hz), 7.348 (td, 1H, J = 1.6 Hz, 7.6 Hz), 7.292–7.210 (m, 3H), 6.884 (d, 1H, J = 15.6 Hz); ^{13}C NMR ($CDCl_3$, 100 MHz) δ: 167.068, 164.521, 138.630, 136.555, 136.523, 135.402, 132.123, 130.830, 130.734, 130.640, 130.496, 130.030, 128.375, 127.357, 116.905, 116.680; MS-ESI m/z: 297.00 $[M + H]^+$; Purity: 96.57%, t_R = 6.15 min (20% water in methanol)%.

*4.1.3.37. (E)-1-(2-((4-fluorophenyl)sulfonyl)vinyl)-2-methylbenzene (**8c**).* **4c** (310 mg, 1 mmol), **5c** (0.13 mL, 1.1 mmol), and *n*-BuLi (c = 2 M, 0.6 mL, 1.2 mmol) gave 237 mg of **8c** as a colorless solid; Yield: 85.8%; mp: 76–77 °C; ^{1}H NMR ($CDCl_3$, 400 MHz) δ: 7.987–7.940 (m, 3H), 7.438 (d, 1H, J = 8 Hz), 7.311 (td, 1H, J = 1.2 Hz, 7.6 Hz), 7.252–7.178 (m, 4H), 6.766 (d, 1H, J = 15.2 Hz), 2.462 (s, 3H); ^{13}C NMR ($CDCl_3$, 100 MHz) δ: 166.772, 164.231, 140.170, 138.206, 136.754, 136.723, 131.049, 130.997, 130.531, 130.436, 127.877, 126.839, 126.493, 116.727, 116.502, 19.709; MS-ESI m/z: 277.05 $[M + H]^+$; Purity: 99.70%, t_R = 6.07 min (20% water in methanol).

*4.1.3.38. (E)-1-chloro-2-(2-((4-fluorophenyl)sulfonyl)vinyl)benzene (**8d**).* **4c** (310 mg, 1 mmol), **5d** (150 mg, 1.1 mmol), and *n*-BuLi (c = 2 M, 0.6 mL, 1.2 mmol) gave 254 mg of **8d** as a white solid; Yield: 86.8%; mp: 98–100 °C; ^{1}H NMR ($CDCl_3$, 400 MHz) δ: 7.984–7.935 (m, 2H), 7.876 (d, 1H, J = 15.6 Hz), 7.427–7.368 (m, 2H), 7.236–7.179 (m, 2H), 7.065 (d, 1H, J = 15.2 Hz), 6.985–6.913 (m. 2H), 3.883 (s, 3H); ^{13}C NMR ($CDCl_3$, 100 MHz) δ: 166.573, 164.036, 158.736, 138.607, 137.170, 137.139, 132.635, 130.780, 130.366, 130.271, 127.522, 120.799, 120.706, 116.538, 116.313, 111.202, 55.432; MS-ESI m/z: 293.00 $[M + H]^+$; Purity: 95.49%, t_R = 5.76 min (20% water in methanol).

*4.1.3.39. (E)-1-(2-((4-fluorophenyl)sulfonyl)vinyl)-3-(trifluoromethyl) benzene (**8e**).* **4c** (310 mg, 1 mmol), **5e** (192 mg, 1.1 mmol), and *n*-BuLi (c = 2 M, 0.6 mL, 1.2 mmol) gave 285 mg of **8e** as a white solid; Yield: 86.5%; mp: 106–107 °C; ^{1}H NMR ($CDCl_3$, 400 MHz) δ: 8.004–7.955 (m, 2H), 7.735–7.660 (m, 4H), 7.550 (t, 1H, J = 8 Hz), 7.277–7.220 (m, 2H), 6.933 (d, 1H, J = 15.2 Hz); ^{13}C NMR ($CDCl_3$, 100 MHz) δ: 167.196, 164.646, 140.815, 136.388, 136.357, 133.174, 132.310, 131.984, 131.858, 131.658, 131.331, 130.873, 130.777, 129.888, 129.413, 127.838, 127.803, 127.766, 127.728, 125.177, 125.139, 125.100, 125.015, 122.306, 119.596, 117.033, 116.807; MS-ESI m/z: 331.20 $[M + H]^+$; Purity: 99.62%, t_R = 6.10 min (20% water in methanol).

*4.1.3.40. (E)-1-(2-((4-fluorophenyl)sulfonyl)vinyl)-3-methoxybenzene (**8f**).* **4c** (310 mg, 1 mmol), **5f** (0.13 mL, 1.1 mmol), and *n*-BuLi (c = 2 M, 0.6 mL, 1.2 mmol) gave 241 mg of **8f** as a white solid; Yield: 81.5%; mp: 105–107 °C; ^{1}H NMR ($CDCl_3$, 400 MHz) δ: 7.988–7.938 (m, 2H), 7.618 (d, 1H, J = 15.6 Hz), 7.473 (s, 1H), 7.412–7.322 (m, 3H), 7.260–7.210 (m, 2H), 6.858 (d, 1H, J = 15.6 Hz); ^{13}C NMR ($CDCl_3$, 100 MHz) δ: 167.122, 164.573, 141.035, 136.522, 136.490, 135.283, 134.107, 131.287, 130.799, 130.704, 130.499, 128.819, 128.317, 126.975, 116.978, 116.753; MS-ESI m/z: 297.00 $[M + H]^+$; Purity: 98.38%, t_R = 6.22 min (20% water in methanol).

*4.1.3.41. (E)-1-(2-((4-fluorophenyl)sulfonyl)vinyl)-3-methylbenzene (**8 g**).* **4c** (310 mg, 1 mmol), **5 g** (0.13 mL, 1.1 mmol), and *n*-BuLi (c = 2 M, 0.6 mL, 1.2 mmol) gave 247 mg of **8 g** as a colorless solid; Yield: 89.3%; mp: 55–57 °C; ^{1}H NMR ($CDCl_3$, 400 MHz) δ: 7.987–7.949 (m, 3H), 7.437 (d, 1H, J = 8 Hz), 7.331–7.291 (m, 1H), 7.252–7.177 (m, 4H), 6.764 (d, 1H, J = 15.2 Hz), 2.462 (s, 3H); ^{13}C NMR ($CDCl_3$, 100 MHz) δ: 166.891, 164.347, 142.913, 138.926, 137.052, 137.022, 132.246, 132.210, 130.580, 130.484, 129.213, 129.045, 126.979, 125.918, 116.756, 116.531, 21.276; MS-ESI m/z: 277.00 $[M + H]^+$; Purity: 98.98%, t_R = 6.21 min (20% water in methanol).

*4.1.3.42. (E)-1-chloro-3-(2-((4-fluorophenyl)sulfonyl)vinyl)benzene (**8 h**).* **4c** (310 mg, 1 mmol), **5 h** (150 mg, 1.1 mmol), and *n*-BuLi (c = 2 M, 0.6 mL, 1.2 mmol) gave 257 mg of **8 h** as a colorless solid; Yield: 88.1%; mp: 66–68 °C; ^{1}H NMR ($CDCl_3$, 400 MHz) δ: 7.988–7.939 (m, 2H), 7.646 (d, 1H, J = 15.6 Hz), 7.310 (t, 1H, J = 8 Hz), 7.253–7.195 (m, 2H), 7.077 (d, 1H, J = 8 Hz), 6.986–6.955 (m, 2H), 6.833 (d, 1H, J = 15.2 Hz), 3.0.815 (s, 3H); ^{13}C NMR ($CDCl_3$, 100 MHz) δ: 166.876, 164.333, 160.007, 142.636, 136.842, 136.811, 133.543, 130.582, 130.487, 130.148, 127.433, 121.270, 117.261, 116.760, 116.535, 113.440, 55.375; MS-ESI m/z: 293.05 $[M + H]^+$; Purity: 98.85%, t_R = 5.57 min (20% water in methanol).

*4.1.3.43. (E)-1-chloro-4-(2-((4-fluorophenyl)sulfonyl)vinyl)benzene (**8i**).* **4c** (310 mg, 1 mmol), **5i** (0.16 mL, 1.1 mmol), and *n*-BuLi (c = 2 M, 0.6 mL, 1.2 mmol) gave 273 mg of **8i** as a white solid; Yield: 82.7%; mp: 136–137 °C; ^{1}H NMR ($CDCl_3$, 400 MHz) δ: 7.995–7.962 (m, 2H), 7.724–7.590 (m, 5H), 7.272–7.230 (m, 2H), 6.935 (d, 1H, J = 15.6 Hz); ^{13}C NMR ($CDCl_3$, 100 MHz) δ: 167.207, 164.655, 140.735, 136.297, 136.265, 135.705, 132.988, 132.660, 130.881, 130.785, 129.939,

128.898, 126.257, 126.219, 126.182, 126.143, 125.034, 122.327, 117.048, 116.823; MS-ESI *m/z*: 331.25 $[M + H]^+$; Purity: 99.52%, t_R = 5.80 min (20% water in methanol).

*4.1.3.44. (E)-1-fluoro-4-((4-(trifluoromethyl)styryl)sulfonyl)benzene (**8j**).* **4c** (310 mg, 1 mmol), **5j** (155 mg, 1.1 mmol), and *n*-BuLi (c = 2 M, 0.6 mL, 1.2 mmol) gave 258 mg of **8j** as a white solid; Yield: 87.2%; mp: 132–133 °C; ^{1}H NMR ($CDCl_3$, 400 MHz) δ: 7.983–7.934 (m, 2H), 7.629 (d, 1H, J = 15.2 Hz), 7.431–7.363 (m, 4H), 7.253–7.203 (m, 2H), 6.817 (d, 1H, J = 15.6 Hz); ^{13}C NMR ($CDCl_3$, 100 MHz) δ: 167.089, 164.542, 141.285, 137.523, 136.676, 136.644, 130.816, 130.750, 130.654, 129.894, 129.568, 127.821, 116.961, 116.736; MS-ESI *m/z*: 297.00 $[M + H]^+$; Purity: 99.86%, t_R = 5.87 min (20% water in methanol).

*4.1.3.45. (E)-1-fluoro-4-((4-methoxystyryl)sulfonyl)benzene (**8 k**).* **4c** (310 mg, 1 mmol), **5 k** (0.13 mL, 1.1 mmol), and *n*-BuLi (c = 2 M, 0.6 mL, 1.2 mmol) gave 267 mg of **8 k** as a white solid; Yield: 96.2%; mp: 112–113 °C; ^{1}H NMR ($CDCl_3$, 400 MHz) δ: 7.980–7.931 (m, 2H), 7.649 (d, 1H, J = 15.2 Hz), 7.379 (d, 2H, J = 8.4 Hz), 7.237–7.193 (m, 4H), 6.780 (d, 1H, J = 15.2 Hz), 2.375 (s, 3H); ^{13}C NMR ($CDCl_3$, 100 MHz) δ: 166.905, 164.364, 142.839, 142.121, 137.132, 137.100, 130.583, 130.488, 129.944, 129.562, 128.721, 125.968, 116.796, 116.571, 21.638; MS-ESI *m/z*: 277.00 $[M + H]^+$; Purity: 99.69%, t_R = 6.05 min (20% water in methanol).

*4.1.3.46. (E)-1-fluoro-4-((4-methylstyryl)sulfonyl)benzene (**8 l**).* **4c** (310 mg, 1 mmol), **5 l** (0.14 mL, 1.1 mmol), and *n*-BuLi (c = 2 M, 0.6 mL, 1.2 mmol) gave 270 mg of **8 l** as a white solid; Yield: 92.4%; mp: 118–119 °C; ^{1}H NMR ($CDCl_3$, 400 MHz) δ: 7.920–7.871 (m, 2H), 7.571 (d, 1H, J = 15.6 Hz), 7.380 (d, 2H, J = 8.4 Hz), 7.208–7.125 (m, 2H), 6.848 (d, 2H, J = 8.8 Hz), 6.635 (d, 1H, J = 15.2 Hz), 3.780 (s, 3H); ^{13}C NMR ($CDCl_3$, 100 MHz) δ: 166.734, 164.196, 162.199, 142.499, 137.345, 137.313, 130.467, 130.397, 130.302, 124.843, 124.302, 116.664, 116.439, 114.584, 55.467; MS-ESI *m/z*: 293.05 $[M + H]^+$; Purity: 99.02%, t_R = 5.32 min (20% water in methanol).

*4.1.3.47. (E)-1-methyl-4-(styrylsulfonyl)benzene (**8 m**).* **4c** (310 mg, 1 mmol), **5 m** (0.12 mL, 1.1 mmol), and *n*-BuLi (c = 2 M, 0.6 mL, 1.2 mmol) gave 267 mg of **8 m** as a colorless solid; Yield: 91.4%; mp: 77–79 °C; ^{1}H NMR ($CDCl_3$, 400 MHz) δ: 7.988–7.939 (m, 2H), 7.685 (d, 1H, J = 15.6 Hz), 7.500–7.477 (m, 2H), 7.449–7.374 (m, 3H), 7.253–7.196 (m, 2H), 6.845 (d, 1H, J = 15.6 Hz); ^{13}C NMR ($CDCl_3$, 100 MHz) δ: 166.944, 164.400, 142.739, 136.958, 136.925, 132.313, 131.395, 130.628, 130.533, 129.186, 128.675, 127.258, 116.809, 116.584; MS-ESI *m/z*: 293.05 $[M + H]^+$; Purity: 98.96%, t_R = 5.11 min (20% water in methanol).

*4.1.3.48. (E)-1-bromo-2-(2-((2-chlorophenyl)sulfonyl)vinyl)benzene (**9a**).* **4d** (327 mg, 1 mmol), **5n** (0.12 mL, 1.1 mmol), and *n*-BuLi (c = 2 M, 0.6 mL, 1.2 mmol) gave 266 mg of **9a** as a colorless solid; Yield: 89.7%; mp: 101–102 °C; ^{1}H NMR ($CDCl_3$, 400 MHz) δ: 8.225 (dd, 1H, J = 1.6 Hz, 8 Hz), 7.851 (d, 1H, J = 15.6 Hz), 7.576–7.387 (m, 5H), 7.234 (d, 1H, J = 15.6 Hz), 7.209–7.098 (m, 2H); ^{13}C NMR ($CDCl_3$, 100 MHz) δ: 162.751, 160.211, 138.174, 138.150, 137.935, 134.691, 133.095, 133.007, 132.722, 131.892, 130.718, 130.313, 130.288, 128.144, 128.060, 127.503, 124.776, 124.740, 120.487, 120.374, 116.463, 116.248; MS-ESI *m/z*: 297.00 $[M + H]^+$; Purity: 98.75%, t_R = 6.61 min (20% water in methanol).

*4.1.3.49. (E)-1-chloro-2-((2-fluorostyryl)sulfonyl)benzene (**9b**).* **4d** (327 mg, 1 mmol), **5b** (0.13 mL, 1.1 mmol), and *n*-BuLi (c = 2 M, 0.6 mL, 1.2 mmol) gave 299 mg of **9b** as a colorless solid; Yield: 95.8%; mp: 71–72 °C; ^{1}H NMR ($CDCl_3$, 400 MHz) δ: 8.232 (d, 1H, J = 7.6 Hz), 8.186 (d, 1H, J = 15.2 Hz), 7.581–7.430 (m, 5H), 7.374–7.269 (m, 2H), 7.052 (d, 1H, J = 15.2 Hz); ^{13}C NMR ($CDCl_3$, 100 MHz) δ: 141.008, 137.657, 135.145, 134.735, 132.551, 132.124, 131.820, 130.643, 130.393, 130.214, 128.302, 127.890, 127.463, 127.261; MS-ESI *m/z*: 313.05 $[M + H]^+$; Purity: 99.50%, t_R = 7.54 min (20% water in methanol).

*4.1.3.50. (E)-1-chloro-2-(2-((2-chlorophenyl)sulfonyl)vinyl)benzene (**9c**).* **4d** (327 mg, 1 mmol), **5o** (0.13 mL, 1.1 mmol), and *n*-BuLi (c = 2 M, 0.6 mL, 1.2 mmol) gave 330 mg of **9c** as a colorless solid; Yield: 92.6%; mp: 77–78 °C; ^{1}H NMR ($CDCl_3$, 400 MHz) δ: 8.235 (dd, 1H, J = 1.6 Hz, 8 Hz), 8.166 (d, 1H, J = 15.6 Hz), 7.635 (dd, 1H, J = 1.2 Hz, 8 Hz), 7.583–7.461 (m, 4H), 7.334 (td, 1H, J = 0.8 Hz, 8 Hz), 7.290–7.247 (m, 1H), 7.039 (d, 1H, J = 15.2 Hz); ^{13}C NMR ($CDCl_3$, 100 MHz) δ: 143.806, 137.885, 134.806, 133.677, 132.835, 132.523, 132.308, 131.971, 130.866, 128.490, 128.232, 127.964, 127.561, 125.688; MS-ESI *m/z*: 356.90 $[M + H]^+$; Purity: 99.46%, t_R = 7.82 min (20% water in methanol).

*4.1.3.51. (E)-1-bromo-2-(2-((2-methoxyphenyl)sulfonyl)vinyl)benzene (**10a**).* **4e** (327 mg, 1 mmol), **5n** (0.12 mL, 1.1 mmol), and *n*-BuLi (c = 2 M, 0.6 mL, 1.2 mmol) gave 266 mg of **10a** as a white solid; Yield: 91.2%; mp: 108–109 °C; ^{1}H NMR ($CDCl_3$, 400 MHz) δ: 8.028 (dd, 1H, J = 1.6 Hz, 8 Hz), 7.786 (d, 1H, J = 15.6 Hz), 7.596–7.552 (m, 1H), 7.483 (td, 1H, J = 2 Hz, 7.6 Hz), 7.417–7.360 (m, 1H), 7.270 (d, 1H, J = 15.6 Hz), 7.176 (td, 1H, J = 1.2 Hz, 7.6 Hz), 7.135–7.085 (m, 2H), 7.017 (d, 1H, J = 8.4 Hz), 3.969 (s, 3H); ^{13}C NMR ($CDCl_3$, 100 MHz) δ: 162.786, 160.252, 157.458, 136.455, 136.430, 135.574, 132.624, 132.536, 130.151, 130.124, 129.914, 129.833, 129.601, 128.478, 124.754, 124.717, 121.126, 121.010, 120.806, 116.503, 116.288, 112.520, 56.303; MS-ESI *m/z*: 293.00 $[M + H]^+$; Purity: 99.70%, t_R = 5.38 min (20% water in methanol).

*4.1.3.52. (E)-1-chloro-2-(2-((2-methoxyphenyl)sulfonyl)vinyl)benzene (**10b**).* **4e** (327 mg, 1 mmol), **5b** (0.13 mL, 1.1 mmol), and *n*-BuLi (c = 2 M, 0.6 mL, 1.2 mmol) gave 299 mg of **10b** as a white solid; Yield: 97.4%; mp: 115–116 °C; ^{1}H NMR ($CDCl_3$, 400 MHz) δ: 8.112 (d, 1H, J = 15.6 Hz), 8.041 (dd, 1H, J = 2 Hz, 8 Hz), 7.603–7.543 (m, 2H), 7.432 (dd, 1H, J = 1.6 Hz, 8 Hz), 7.336 (td, 1H, J = 1.6 Hz, 7.6 Hz), 7.291 (dd, 1H, J = 1.6 Hz, 7.6 Hz), 7.134–7.090 (m, 2H), 7.018 (d, 1H, J = 8.4 Hz), 3.978 (s, 3H); ^{13}C NMR ($CDCl_3$, 100 MHz) δ: 157.494, 139.469, 135.671, 135.204, 131.802, 131.225, 130.391, 129.742, 129.698, 128.341, 128.204, 127.314, 120.799, 112.493, 56.340; MS-ESI *m/z*: 309.00 $[M + H]^+$; Purity: 99.72%, t_R = 6.02 min (20% water in methanol).

*4.1.3.53. (E)-1-fluoro-2-(2-((2-methoxyphenyl)sulfonyl)vinyl)benzene (**10c**).* **4e** (327 mg, 1 mmol), **5o** (0.13 mL, 1.1 mmol), and *n*-BuLi (c = 2 M, 0.6 mL, 1.2 mmol) gave 341 mg of **10c** as a white solid; Yield: 96.6%; mp: 114–115 °C; ^{1}H NMR ($CDCl_3$, 400 MHz) δ: 8.081 (d, 1H, J = 15.2 Hz), 8.043 (dd, 1H, J = 1.6 Hz, 8 Hz), 7.626 (dd, 1H, J = 1.2 Hz, 8 Hz), 7.605–7.534 (m, 2H), 7.328 (td, 1H, J = 1.2 Hz, 7.6 Hz), 7.271–7.229 (m, 1H), 7.132–7.091 (m, 1H), 7.065 (d, 1H, J = 15.6 Hz), 7.019 (d, 1H, J = 8.4 Hz), 3.986 (s, 3H); ^{13}C NMR ($CDCl_3$, 100 MHz) δ: 157.197, 141.455, 135.572, 133.319, 132.470, 131.824, 129.463, 129.285, 128.121, 127.780, 127.678, 125.175, 120.480, 112.358, 56.175; MS-ESI *m/z*: 352.95 $[M + H]^+$; Purity: 99.80%, t_R = 6.19 min (20% water in methanol).

4.2. Biological studies

4.2.1. Cell culture

The PC12 cell line was purchased from the Shanghai Institute of Biochemistry and Cell Biology, Chinese Academy of Sciences. It was cultured in Dulbecco's modified Eagle's medium containing 10% FBS, 2 mM glutamine, and 100 units/mL penicillin/streptomycin, and was maintained at 37 °C in a humidified incubator with 5% CO_2.

4.2.2. MTT assay

The PC12 cells were seeded to adhere for 24 h, and addition of target compounds (10 μM, 20 μM and 50 μM) was followed. After 24 h the cell survival was determined by MTT assay. For the H_2O_2 injury cellular model, PC12 cells were grown to adhere for 24 h and addition of target compounds of indicated concentrations was followed. After 24 h the cells were damaged by H_2O_2 (500 μM) for 12 h followed by MTT assay. The more detailed information on the procedure was based on our previous work [39–41].

4.2.3. LDH leakage determination

PC12 cells were seeded to adhere for 24 h, and then the cells were incubated with **9b** (0.5 μM and 1 μM) and **9c** (0.5 μM and 1 μM) for 24 h. Afterwards, the old culture mediums were replaced with newly prepared medium having 500 μM H_2O_2, and the cells were cultured for additional 12 h. Then measurement of LDH activity was conducted. The more detailed information on the procedure was based on our previous work [39–41].

4.2.4. Determination of the cellular ROS level

PC12 cells were bred to adhere for 24 h and then the cells were incubated with **9b** (0.5 μM and 1 μM) and **9c** (0.5 μM and 1 μM) for 24 h. Afterwards 500 μM H_2O_2 was added and the cells were incubated for 5 h. After the culture medium was discarded, 10 μM DCFH-DA in fresh FBS-free medium was added, the culture mixture of which was maintained at 37 °C for 30 min in dark. Afterwards, photos were obtained by using fluorescence microscope (Life Technology).

4.2.5. Real-time quantitative reverse transcription-polymerase chain reaction (qRT-PCR)

PC12 cells were bred to adhere for 24 h followed by incubation of **9b** (1 μM) and **9c** (1 μM) for indicated time. The treated cells at the indicated time were used to extract the total RNA by using RNA extraction kit (TaKaRa, China). Reverse transcription kit (TaKaRa, China) was exploited to reversely transcribe the extracted RNA to cDNA. PCR Master Mix (TaKaRa, China) was utilized for qRT-PCR analysis on the Mx3005P RT-PCR system (Agilent Technologies). The sequences of genes primers were the same as we used before [39–41].

4.2.6. Assessment of content of GSH, and activity of TrxR, NQO1, and HO-1

PC12 cells were bred to adhere for 24 h, and then they were incubated with **9b** (0.5 μM and 1 μM) or **9c** (0.5 μM and 1 μM) for 24 h. Then the cells were collected and lysed to prepare cellular extracts for each antioxidant species determination. The detailed information on the procedure was based on our previous work [39–41].

For the determination of total GSH, an enzymatic method was employed. Briefly, a solution (120 μL) of DTNB (0.33 mg/mL) and glutathione reductase (1.66 units/mL) was added to each cellular sample (20 μL) followed by addition of NADPH (60 μL of 0.66 mg/mL). And the same amount of DMSO was added to the control. Then the absorbance of 412 nm was determined every 10 s for 2 min.

For the evaluation of cellular TrxR activity, the endpoint insulin reduction assay was conducted and the total protein content was quantified by Bradford method. Briefly, the cellular samples containing 20 μg of total proteins was incubated with Tris–HCl (100 mM, pH 7.6), insulin (0.3 mM), NADPH (660 μM), EDTA (3 mM), and *E. coli* Trx (15 μM) in a final volume of 50 μL at 37 °C for 30 min. Then 200 μL of DTNB (1 mM in 6 M guanidine hydrochloride, pH 8.0) was used to terminate the reaction. The blank group was treated in the same manner without addition of Trx, and the same amount of DMSO was added to the control group. Then the absorbance of 412 nm was determined, and the blank value was subtracted from the experimental group. The TrxR activity was expressed as the percentage of the control.

For the determination of cellular NQO1 activity, a spectrophotometric method using 2, 6-dichlorophenol-indophenol (DCPIP) as an electron acceptor in the reduction assay was employed by measuring the absorbance at 600 nm and the total protein content was quantified by Bradford method. Briefly, the reduction assay was conducted by mixing the cell samples (5 μg of total proteins), NADH (200 μM), Tris–HCl (20 mM, pH 7.4), and DCPIP (40 μM), with/without addition of 20 μM dicoumarol (a selective inhibitor of NQO1). Then absorbance decrease at 600 nm was determined every 8 s for 2 min at room temperature. The NQO1 activity was calculated by using the dicoumarol-inhibitable part of DCPIP reduction. The same amount of DMSO was added to the control group and the NQO1 activity was expressed as the percentage of the control.

For the evaluation of cellular HO-1 activity, a spectrophotometric method was employed and the total protein content was quantified by Bradford method. Briefly, the cellular samples was added to buffer A consisting of sucrose (0.25 M), Tris-HCl (20 mM, pH 7.4), phenylmethylsulfonyl fluoride (1 mM), and Na_3VO_4 (1 mM). Then the cellular samples containing 50 μg of total proteins was incubated with NADPH (1 mM), hemin (25 μM), and excessive bovine liver extracts (lysed in buffer A containing biliverdin reductase) in a final volume of 100 μL at 37 °C for 30 min in dark. The blank group was treated in the same manner without addition of NADPH, and the same amount of DMSO was added to the control group. Then the absorbance of 464 nm was determined, and the HO-1 activity was expressed as the percentage of the control.

4.2.7. Cellular TrxR activity determination by TRFS-Green

PC12 cells were bred to adhere for 24 h, and then were treated with **9b** (0.5 μM and 1 μM) and **9c** (0.5 μM and 1 μM) for further 24 h followed by addition of 10 μM TRFS-Green. 4 h later, the activity of TrxR was determined and the photos were taken from a fluorescence microscope (Life Technology).

4.2.8. Western blots analysis

The PC12 cells were treated with **9b** (1 μM) and **9c** (1 μM) for 24 h, and then the cellular fractions from nuclei, cytoplasm and whole cells were prepared following our published procedures [39–41]. The protein expression levels were determined by standard Western blots analysis. Briefly, the whole cell fraction was prepared by lysing PC12 cells with RIPA buffer. The cellular fractions from nuclei and cytoplasm were obtained by lysing PC12 cells with buffer A containing Hepes (10 mM, pH 7.9), KCl (10 mM), EDTA (0.1 mM), EGTA (0.1 mM), DTT (1 μM), followed by addition of 1 μM of protease inhibitor cocktail. 15 min later, Nonidet-P40 (10 μM) was added, and the mixture was vortexed for 15 s, followed by centrifugation for 10 min (1000 *g*, 4 °C). Thereafter, the cellular nuclear fractions were separated from the cytosolic part. The pellet was resuspended in 100 μM of buffer B containing Hepes (20 mM, pH 7.9), NaCl (0.4 M), EDTA (1 mM), EGTA (1 mM), DTT (1 μM), followed by addition of 1 μM of protease inhibitor cocktail. After incubation on ice for 15 min, the mixture was vortexed for 15 s every 2 min, followed by centrifugation for 10 min (20000 *g*, 4 °C), and the supernatant was collected as the cellular nuclear fractions. The total protein content was quantified by Bradford method, and the protein samples were loaded on SDS-PAGE for electrophoresis. Then the separated proteins were transferred on PVDF membranes, followed by blocking with 5% nonfat milk for 1 h at room temperature. Afterwards the PVDF membranes were incubated with primary antibodies overnight at 4 °C, and then they were incubated with corresponding secondary antibodies for 1 h at room temperature. Subsequently, they were incubated with the enhanced chemiluminescence kit, and the bands were recorded and the intensities were analyzed.

4.2.9. Establishment of Nrf2 knockdown PC12 cell line

The detailed information for the generation of stable Nrf2 knockdown PC12 cells were in the light of the methods published by our group [39–41]. In short, mice *Nrf2* gene was specifically interfered with sh*Nrf2-842*, and sh*NT* was used as a control. G418 (0.5 mg/mL) was

used to screened to generate stable PC12-sh*Nrf2* cells and PC12-sh*NT* cells.

4.2.10. *ARE-luciferase reporter gene assay*

This experiment was in accordance with the method established in our recent published paper [38]. In a word, PC12 cells were transfected with the p*ARE*-luciferase plasmid (Beyotime, China), and then they were screened with G418 (0.5 mg/mL) to generate a stable transfected cell line. *t*-BHQ (20 μM and 40 μM, utilized as a positive control), **9b** (0.5 μM and 1 μM), and **9c** (0.5 μM and 1 μM) were added to incubate with the transfected cells for 24 h followed by preparation of cell samples. The luciferase activity was determined with the aid of Firefly Luciferase Reporter Gene Assay Kit (Beyotime, China).

4.2.11. *Statistics*

Student's *t*-test was used to check the difference between two groups, and differences among multiple groups were checked by one-way analysis of variance. Data are expressed as means ± standard deviation (SD). It was considered to be statistically significant when P value is < 0.05.

Declaration of Competing Interest

The authors declare that they have no known competing financial interests or personal relationships that could have appeared to influence the work reported in this paper.

Acknowledgements

Financial supports from the National Natural Science Foundation of China (21778028, 22077055), the Natural Science Foundation of Gansu Province (20JR5RA311, 18JR4RA003), and the 111 project are acknowledged.

Appendix A. Supplementary data

Supplementary data to this article can be found online at https://doi.org/10.1016/j.bioorg.2020.104520.

References

[1] B.C. Dickinson, C.J. Chang, Chemistry and biology of reactive oxygen species in signaling or stress responses, Nat. Chem. Biol. 7 (2011) 504–511.
[2] M.P. Murphy, A. Holmgren, N.G. Larsson, B. Halliwell, C.J. Chang, B. Kalyanaraman, S.G. Rhee, P.J. Thornalley, L. Partridge, D. Gems, T. Nystrom, V. Belousov, P.T. Schumacker, C.C. Winterbourn, Unraveling the biological roles of reactive oxygen species, Cell Metab. 13 (2011) 361–366.
[3] K.M. Holmstrom, T. Finkel, Cellular mechanisms and physiological consequences of redox-dependent signalling, Nat. Rev. Mol. Cell Biol. 15 (2014) 411–421.
[4] T. Finkel, N.J. Holbrook, Oxidants, oxidative stress and the biology of ageing, Nature 408 (2000) 239–247.
[5] K.J. Barnham, C.L. Masters, A.I. Bush, Neurodegenerative diseases and oxidative stress, Nat. Rev. Drug Discov. 3 (2004) 205–214.
[6] M. Rojo de la Vega, E. Chapman, D.D. Zhang, NRF2 and the Hallmarks of Cancer, Cancer Cell 34 (2018) 21–43.
[7] J. Gracia-Sancho, M.J. Salvadó, Gastrointestinal Tissue: Oxidative Stress and Dietary Antioxidants, Academic Press, 2017.
[8] T.R. Dugas, Unraveling mechanisms of toxicant-induced oxidative stress in cardiovascular disease, Curr. Opin. Toxicol. 7 (2018) 1–8.
[9] J.N. Cobley, M.L. Fiorello, D.M. Bailey, 13 reasons why the brain is susceptible to oxidative stress, Redox Biol. 15 (2018) 490–503.
[10] H.E. de Vries, M. Witte, D. Hondius, A.J. Rozemuller, B. Drukarch, J. Hoozemans, J. van Horssen, Nrf2-induced antioxidant protection: a promising target to counteract ROS-mediated damage in neurodegenerative disease? Free Radical Biol. Med. 45 (2008) 1375–1383.
[11] R. Franco, J.A. Doorn, J.-C. Rochet, Oxidative stress and redox signalling in Parkinson's disease, Royal Society of Chemistry, 2017.
[12] S. Fahn, G. Cohen, The oxidant stress hypothesis in Parkinson's disease: evidence supporting it, Ann. Neurol. 32 (1992) 804–812.
[13] F.L. van Muiswinkel, H.B. Kuiperij, The Nrf2-ARE Signalling Pathway: Promising Drug Target to Combat Oxidative Stress in Neurodegenerative Disorders, Curr. Drug Targets: CNS Neurol. Disord. 4 (2005) 267–281.
[14] P.C. Trippier, K. Jansen Labby, D.D. Hawker, J.J. Mataka, R.B. Silverman, Target- and mechanism-based therapeutics for neurodegenerative diseases: strength in numbers, J. Med. Chem. 56 (2013) 3121–3147.
[15] C.J. Schmidlin, M.B. Dodson, L. Madhavan, D.D. Zhang, Redox regulation by NRF2 in aging and disease, Free Radical Biol. Med. 134 (2019) 702–707.
[16] M.J. Calkins, D.A. Johnson, J.A. Townsend, M.R. Vargas, J.A. Dowell, T. P. Williamson, A.D. Kraft, J.M. Lee, J. Li, J.A. Johnson, The Nrf2/ARE pathway as a potential therapeutic target in neurodegenerative disease, Antioxid. Redox Signaling 11 (2009) 497–508.
[17] A. Cuadrado, P. Moreno-Murciano, J. Pedraza-Chaverri, The transcription factor Nrf2 as a new therapeutic target in Parkinson's disease, Expert Opin. Ther. Targets 13 (2009) 319–329.
[18] S. Magesh, Y. Chen, L. Hu, Small molecule modulators of Keap1-Nrf2-ARE pathway as potential preventive and therapeutic agents, Med. Res. Rev. 32 (2012) 687–726.
[19] M. Dodson, M.R. de la Vega, A.B. Cholanians, C.J. Schmidlin, E. Chapman, D. D. Zhang, Modulating NRF2 in Disease: Timing Is Everything, Annu. Rev. Pharmacol. Toxicol. 59 (2019) 555–575.
[20] C.J. Schmidlin, M.B. Dodson, LalithaMadhavan, D.D. Zhang, Redox regulation by NRF2 in aging and disease, Free Radical Biol. Med. 134 (2019) 702–707.
[21] T. Suzuki, H. Motohashi, M. Yamamoto, Toward clinical application of the Keap1-Nrf2 pathway, Trends Pharmacol. Sci. 34 (2013) 340–346.
[22] A.J. Wilson, J.K. Kerns, J.F. Callahan, C.J. Moody, Keap calm, and carry on covalently, J. Med. Chem. 56 (2013) 7463–7476.
[23] M.C. Lu, J.A. Ji, Z.Y. Jiang, Q.D. You, The Keap1-Nrf2-ARE Pathway As a Potential Preventive and Therapeutic Target: An Update, Med. Res. Rev. 36 (2016) 924–963.
[24] Z.Y. Jiang, M.C. Lu, Q.D. You, Discovery and Development of Kelch-like ECH-Associated Protein 1. Nuclear Factor Erythroid 2-Related Factor 2 (KEAP1:NRF2) Protein-Protein Interaction Inhibitors: Achievements, Challenges, and Future Directions, J. Med. Chem. 59 (2016) 10837–10858.
[25] Z.Y. Jiang, M.C. Lu, Q.D. You, Nuclear Factor Erythroid 2-Related Factor 2 (Nrf2) Inhibition: An Emerging Strategy in Cancer Therapy, J. Med. Chem. 62 (2019) 3840–3856.
[26] J.S. Pallesen, K.T. Tran, A. Bach, Non-covalent Small-Molecule Kelch-like ECH-Associated Protein 1-Nuclear Factor Erythroid 2-Related Factor 2 (Keap1-Nrf2) Inhibitors and Their Potential for Targeting Central Nervous System Diseases, J. Med. Chem. 61 (2018) 8088–8103.
[27] D.D. Zhang, M. Hannink, Distinct cysteine residues in Keap1 are required for Keap1-dependent ubiquitination of Nrf2 and for stabilization of Nrf2 by chemopreventive agents and oxidative stress, Mol. Cell Biol. 23 (2003) 8137–8151.
[28] B. Halliwell, Oxidative stress and neurodegeneration: where are we now? J. Neurochem. 97 (2006) 1634–1658.
[29] B.J.J.o.n. Halliwell, Reactive oxygen species and the central nervous system, J. Neurochem. 59 (1992) 1609–1623.
[30] M. Dodson, R. Castro-Portuguez, D.D. Zhang, NRF2 plays a critical role in mitigating lipid peroxidation and ferroptosis, Redox Biol. 23 (2019).
[31] W. Hur, N.S. Gray, Small molecule modulators of antioxidant response pathway, Curr. Opin. Chem. Biol. 15 (2011) 162–173.
[32] P. Liu, W. Tian, S. Tao, J. Tillotson, E.M.K. Wijeratne, A.A.L. Gunatilaka, D. D. Zhang, E. Chapman, Non-covalent NRF2 Activation Confers Greater Cellular Protection than Covalent Activation, Cell Chem. Biol. 26 (2019) 1427–1435 e1425.
[33] K.M. Lee, T.Y. Kwon, U. Kang, E.K. Seo, J.H. Yun, C.W. Nho, Y.S. Kim, Tussilagonone-induced Nrf2 pathway activation protects HepG2 cells from oxidative injury, Food Chem. Toxicol. 108 (2017) 120–127.
[34] R. Joo Choi, M.S. Cheng, Y. Shik Kim, Desoxyrhapontigenin up-regulates Nrf2-mediated heme oxygenase-1 expression in macrophages and inflammatory lung injury, Redox Biol. 2 (2014) 504–512.
[35] J. Lee, K. Song, E. Huh, M.S. Oh, Y.S. Kim, Neuroprotection against 6-OHDA toxicity in PC12 cells and mice through the Nrf2 pathway by a sesquiterpenoid from Tussilago farfara, Redox Biol. 18 (2018) 6–15.
[36] R.H. Scannevin, S. Chollate, M.Y. Jung, M. Shackett, H. Patel, P. Bista, W. Zeng, S. Ryan, M. Yamamoto, M. Lukashev, K.J. Rhodes, Fumarates promote cytoprotection of central nervous system cells against oxidative stress via the nuclear factor (erythroid-derived 2)-like 2 pathway, J. Pharmacol. Exp. Ther. 341 (2012) 274–284.
[37] Z.L. Song, F. Bai, B. Zhang, J. Fang, Synthesis of Dithiolethiones and Identification of Potential Neuroprotective Agents via Activation of Nrf2-Driven Antioxidant Enzymes, J. Agric. Food Chem. 68 (2020) 2214–2231.
[38] Y. Hou, X. Li, S. Peng, J. Yao, F. Bai, J. Fang, Lipoamide Ameliorates Oxidative Stress via Induction of Nrf2/ARE Signaling Pathway in PC12 Cells, J. Agric. Food Chem. 67 (2019) 8227–8234.
[39] J. Yao, B. Zhang, C. Ge, S. Peng, J. Fang, Xanthohumol, a polyphenol chalcone present in hops, activating Nrf2 enzymes to confer protection against oxidative damage in PC12 cells, J. Agric. Food Chem. 63 (2015) 1521–1531.
[40] J. Yao, C. Ge, D. Duan, B. Zhang, X. Cui, S. Peng, Y. Liu, J. Fang, Activation of the phase II enzymes for neuroprotection by ginger active constituent 6-dehydrogingerdione in PC12 cells, J. Agric. Food Chem. 62 (2014) 5507–5518.
[41] S. Peng, B. Zhang, X. Meng, J. Yao, J. Fang, Synthesis of piperlongumine analogues and discovery of nuclear factor erythroid 2-related factor 2 (Nrf2) activators as potential neuroprotective agents, J. Med. Chem. 58 (2015) 5242–5255.
[42] S. Peng, Y. Hou, J. Yao, J. Fang, Activation of Nrf2 by costunolide provides neuroprotective effect in PC12 cells, Food Funct. 10 (2019) 4143–4152.
[43] S. Peng, Y. Hou, J. Yao, J. Fang, Activation of Nrf2-driven antioxidant enzymes by cardamonin confers neuroprotection of PC12 cells against oxidative damage, Food Funct. 8 (2017) 997–1007.

[44] S. Peng, J. Yao, Y. Liu, D. Duan, X. Zhang, J. Fang, Activation of Nrf2 target enzymes conferring protection against oxidative stress in PC12 cells by ginger principal constituent 6-shogaol, Food Funct. 6 (2015) 2813–2823.
[45] S. Peng, B. Zhang, J. Yao, D. Duan, J. Fang, Dual protection of hydroxytyrosol, an olive oil polyphenol, against oxidative damage in PC12 cells, Food Funct. 6 (2015) 2091–2100.
[46] F. Bai, B. Zhang, Y. Hou, J. Yao, Q. Xu, J. Xu, J. Fang, Xanthohumol Analogues as Potent Nrf2 Activators against Oxidative Stress Mediated Damages of PC12 Cells, ACS Chem. Neurosci. 10 (2019) 2956–2966.
[47] Y. Hou, S. Peng, X. Li, J. Yao, J. Xu, J. Fang, Honokiol Alleviates Oxidative Stress-Induced Neurotoxicity via Activation of Nrf2, ACS Chem. Neurosci. 9 (2018) 3108–3116.
[48] M. Dumont, E. Wille, N.Y. Calingasan, D. Tampellini, C. Williams, G.K. Gouras, K. Liby, M. Sporn, C. Nathan, M. Flint Beal, M.T. Lin, Triterpenoid CDDO-methylamide improves memory and decreases amyloid plaques in a transgenic mouse model of Alzheimer's disease, J. Neurochem. 109 (2009) 502–512.
[49] B. Wei, J. Zhou, J.J. Xu, J. Cui, F.F. Ping, J.J. Ling, Y.J. Chen, Discovery of coumarin-derived imino sulfonates as a novel class of potential cardioprotective agents, Eur. J. Med. Chem. 184 (2019).
[50] R. Kachadourian, B.J. Day, S. Pugazhenti, C.C. Franklin, E. Genoux-Bastide, G. Mahaffey, C. Gauthier, A. Di Pietro, A. Boumendjel, A synthetic chalcone as a potent inducer of glutathione biosynthesis, J. Med. Chem. 55 (2012) 1382–1388.
[51] V. Kumar, S. Kumar, M. Hassan, H. Wu, R.K. Thimmulappa, A. Kumar, S.K. Sharma, V.S. Parmar, S. Biswal, S.V. Malhotra, Novel chalcone derivatives as potent Nrf2 activators in mice and human lung epithelial cells, J. Med. Chem. 54 (2011) 4147–4159.
[52] J.W. Choi, S. Kim, J.H. Park, H.J. Kim, S.J. Shin, J.W. Kim, S.Y. Woo, C. Lee, S. M. Han, J. Lee, A.N. Pae, G. Han, K.D. Park, Optimization of Vinyl Sulfone Derivatives as Potent Nuclear Factor Erythroid 2-Related Factor 2 (Nrf2) Activators for Parkinson's Disease Therapy, J. Med. Chem. 62 (2019) 811–830.
[53] X. Ning, Y. Guo, X. Wang, X. Ma, C. Tian, X. Shi, R. Zhu, C. Cheng, Y. Du, Z. Ma, Z. Zhang, J. Liu, Design, synthesis, and biological evaluation of (e)-3,4-dihydroxystyryl aralkyl sulfones and sulfoxides as novel multifunctional neuroprotective agents, J. Med. Chem. 57 (2014) 4302–4312.
[54] S.Y. Woo, J.H. Kim, M.K. Moon, S.H. Han, S.K. Yeon, J.W. Choi, B.K. Jang, H. J. Song, Y.G. Kang, J.W. Kim, J. Lee, D.J. Kim, O. Hwang, K.D. Park, Discovery of vinyl sulfones as a novel class of neuroprotective agents toward Parkinson's disease therapy, J. Med. Chem. 57 (2014) 1473–1487.
[55] C. Malagelada, L.A. Greene, PC12 cells as a model for Parkinson's disease research (Chapter 29 in Parkinson's Disease), Elsevier, 2008, 375-387.
[56] L. Zhang, D. Duan, Y. Liu, C. Ge, X. Cui, J. Sun, J. Fang, Highly selective off-on fluorescent probe for imaging thioredoxin reductase in living cells, J. Am. Chem. Soc. 136 (2014) 226–233.